

Methodological Investigations Towards the Synthesis of Sesquiterpene-neolignans

James Glen

Thesis submitted to The University of Nottingham for the degree of Master of
Research.

SUPERVISOR: PROF. ROSS DENTON

Acknowledgements

I would like to thank Prof. Ross Denton for giving me the opportunity to carry out research in his group at the University of Nottingham. The support and approachable attitude he exudes has benefited me substantially throughout my project this year. I would like to thank all members of the Denton group for their support and suggestions throughout my time in the laboratory. In particular, I would like to show my utmost appreciation to Val, for his excellent guidance and patience through a very tough year for all in the research community. Starting in the group with minimal practical experience, he has guided me through many tribulations that can arise with the joys of chemistry in a research laboratory. To all my friends and family that have sent me words of encouragement and belief in my abilities, I am forever grateful. To my mother Mary, your patience and kindness have helped me through. To my brother John, the better twin, your actions throughout this year will help me for many to come. To Louisa, your exuberance, kindness and loving motivation have alleviated any doubts I have had about myself and spurred me on through many a tough time this year. Thank you.

Abstract

Lignans and neolignans are a family of compounds from the *illicium* genus. These compounds are derived from the oxidative coupling of the phenolic compound, chavicol. Investigations into the medicinal benefits of this diverse family of compounds are ongoing with promise shown in the growth of neurons and the fight against neurodegenerative diseases. Sesquiterpene-neolignans, a subclass of this family of compounds also show enhanced activity in this therapeutic area. Efficient syntheses of these derivatives are a key topic of research being pursued to enable future structure activity relationship studies to be carried out.

Investigations towards the synthesis of the sesquiterpene-neolignan, monoterpenylmagnolol, have been employed within this thesis. Chemistry successfully utilised in previous syntheses of neolignan derivatives was investigated for compatibility with synthesis of monoterpenylmagnolol. Attempted rhodium catalysed addition of aryl constituents to the conjugated enone, cryptone, yielded inconclusive results. This creates a need for further optimisation of this conjugate addition reaction. In conjunction with this, computational studies into the hypothesised biosynthetic pathway of caryolanemagnolol were implemented. This study validated the theorised phenolic trapping of the caryolane core through a secondary carbocation intermediate.

Abbreviations

°C	degrees Celsius
μM	micro Molar
BBr ₃	boron tribromide
BCl ₃ •SMe ₂	boron trichloride dimethylsulfide complex
CH ₂ Cl ₂	dichloromethane
ChAT	choline acetyltransferase
CHCl ₃	chloroform
CuI	copper iodide
CuTC	copper(I) thiophene-2-carboxylate
d (NMR)	doublet
DBDMH	1,3-dibromo-5,5-Dimethylhydantoin
DCE	1,2-dichloroethane
DCM	dichloromethane
DDQ	2,3-dichloro-5,6-dicyano-1,4-benzoquinone
DHQ	3-dehydroquinone
DIBALH	diisobutylaluminium hydride
DMF	dimethyl formamide
DMSO	dimethylsulfoxide
Dppf	1,1'-bis(diphenylphosphino)ferrocene
Dppp	1,3-bis(diphenylphosphino)propane
e ⁻	electron
EPSP	5-enolpyruvylshikimate-3-phosphate

ESI	electron spray ionization
Et ₂ NTMS	<i>N,N</i> -diethyltrimethylsilylamine
Et ₂ O	diethyl ether
FeCl ₃	iron trichloride
H	hours
H ⁺	proton
HCl	hydrogen chloride
HMPA	hexamethylphosphoramide
HRMS	high resolution mass spectrometry
<i>i</i> PrOH	isopropyl alcohol
IR	infrared
KHF ₂	potassium bifluoride
M	moles
m (NMR)	multiplet
m/z	mass to charge ratio
<i>m</i> -CPBA	3-chloroperbenzoic acid
Me	methyl
MOM	methoxymethyl
MOM-Cl	methoxymethyl chloride
NAD(P)H	nicotinamide adenine dinucleotide (phosphate)
NAD ⁺	nicotinamide adenine dinucleotide
NBS	<i>N</i> -bromo succinimide
NIS	<i>N</i> -iodosuccinimide
NMR	nuclear magnetic resonance

<i>N</i> -PSP	<i>N</i> -phenylselenophthalimide
Pd(OAc) ₂	palladium acetate
Pd(PPh ₃) ₂ Cl ₂	bis(triphenylphosphine)palladium chloride
Pd(PPh ₃) ₄	tetrakis(triphenylphosphine)palladium (0)
Pd ₂ dba ₃	tris(dibenzylideneacetone)dipalladium(0)
Ph	phenyl
<i>p</i> -TSA	<i>p</i> -toluenesulfonic acid
r.t.	room temperature
Red-Al	sodium bis(2-methoxyethoxy)aluminium hydride
s (NMR)	singlet
<i>s</i> -BuLi	secondary butyllithium
t (NMR)	triplet
TAL	tyrosine ammonia lyase
TBAF	tetrabutylammonium fluoride
TBS	tert-butyldimethylsilyl
TBS-Cl	tert-butyldimethylsilyl chloride
<i>t</i> -BuLi	tertiary butyllithium
THF	tetrahydrofuran
V _{max}	absorption maximum
ZnCl ₂	zinc chloride
δ	chemical shift

Contents

Abbreviations	1
1: Introduction	8
1.1 Neolignans and Lignans	8
1.2 Biological pathway of lignans and neolignans and derivatives.....	9
1.3 Biological activity of neurtite outgrowth – Neolignans and their derivatives	13
1.3.1 Neolignans biological activity.....	13
1.3.2 Terpene neolignans biological activity and isolation	14
1.4 Isolation and syntheses of neolignans	17
Magnolol	17
Dunnianol.....	20
Honokiol	21
1.5 Terpene-neolignan syntheses	23
2. Project outline.....	30
3. Results and discussion	32
3.1.1 Construction of the biaryl skeleton	32
3.1.2 Turbo Grignard route.....	32
3.1.3 Ullmann strategy.....	34
3.1.4 Protection and halogenation	35
3.1.5 TBS protection and bromination.....	35
3.1.6 MOM protection and iodination	36
3.2 Cryptone synthesis.....	37
3.2.1 Conjugate addition strategy.....	37
3.2.2 <i>ortho</i> -Methoxyarylation through 1,4-Rhodium Shift.....	38
4. Computational Investigation of Biosynthetic Hypothesis For The Formation of Caryolanemagnolol	41
5. Conclusions	43
6. Future work.....	43
7. Experimental	46
7.1 General Details.....	46
7.2 Synthesis of compounds	47
7.3 Computational data	50
8. References	57

1: Introduction

1.1 Neolignans and Lignans

The naturally occurring phenolic compounds known as lignans and neolignans are found throughout the plant kingdom and can be extracted from various natural sources such as roots, seeds, leaves and fruits of flowering plants¹. They have varying biological activities that contribute to different pharmacological effects within humans such as antitumor, antiviral, antibacterial and anti-inflammatory to name but a few². This has therefore made lignans and their derivatives a key topic of research and the pursuit of various synthetic studies. The work of Siegel's group as an example has looked to isolate the sesquiterpene-neolignan clovanemagnolol and test its neurotrophic activity³. The application of using these lignan and neolignan derivatives as neuronal promoting substances is an area of research that has subsequently led to the substances becoming targets of total syntheses. These syntheses and the corresponding biological pathways are briefly discussed in this review.

The overarching term for the class of compounds is lignan but due to the structural variety with which lignans are found in nature, these can be divided into two main types, classical lignans and neolignans. The classical lignan is made up of two phenylpropane units linked in β - β /8-8' fashion through the C-3 and C-6 of the corresponding units (figure 1). Neolignans are linked dimers through which the linkage is not through an 8-8' coupling. Lignans and neolignans can be divided into a further 6 and 15 subclasses, respectively.

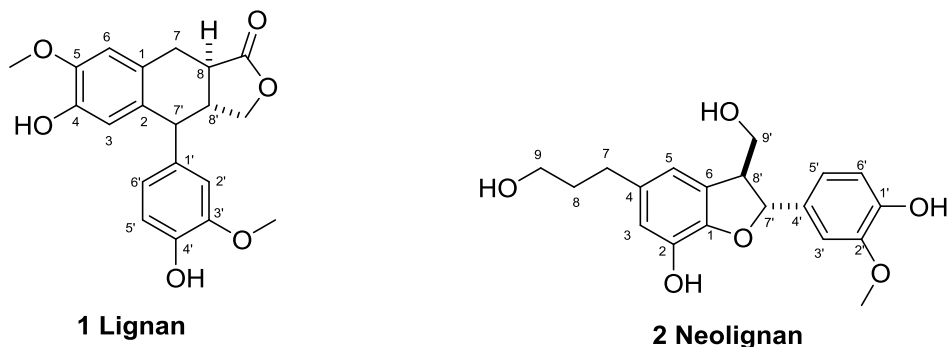


Figure 1- classic lignan and neolignan

1.2 Biological pathway of lignans and neolignans and derivatives.

The lignan and neolignan biological pathway can be derived from the shikimic acid pathway⁴. This pathway leads to the compound 4-coumaric acid (**19**) upon loss of the amine group of *L*-tyrosine (**18**) (scheme 3). When 4-coumaric acid is reduced, this leads to the compound 4-hydroxycinnamyl alcohol, a key building block in the syntheses of neolignans and lignans such as magnolol (**3**), honokiol (**4**) and dunnaniol (**5**).

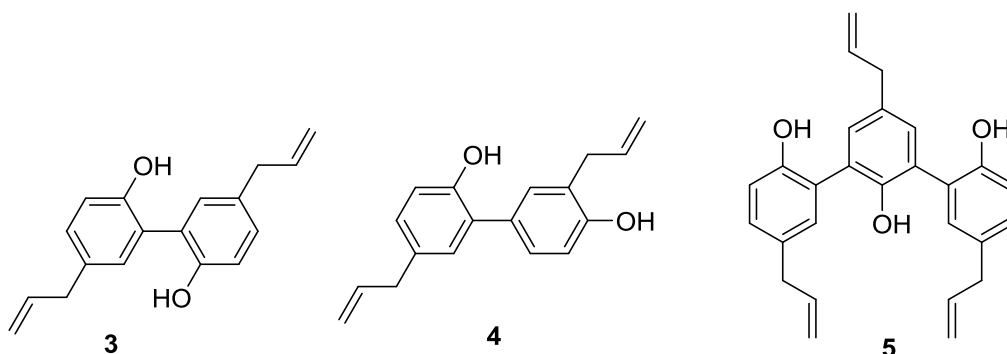
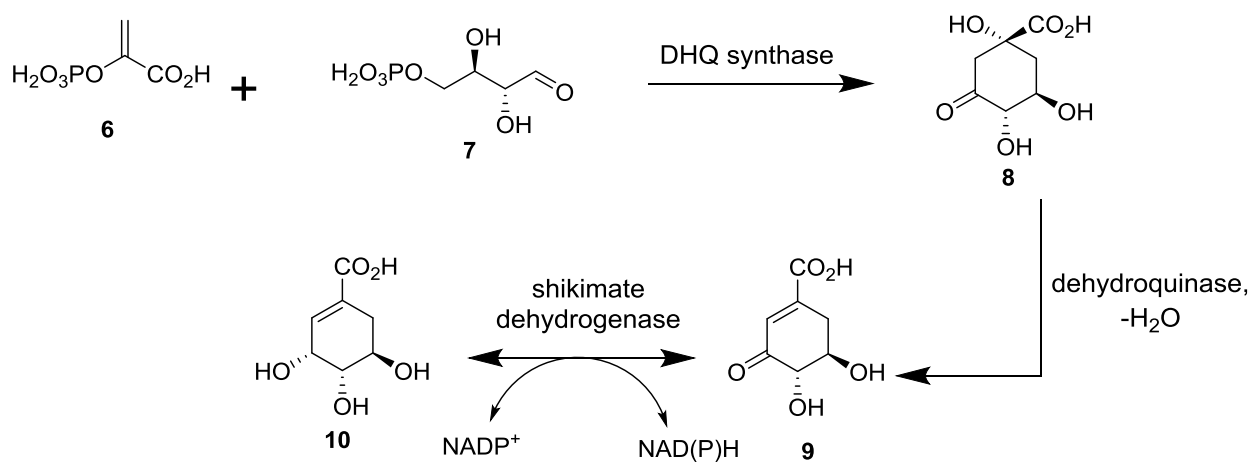


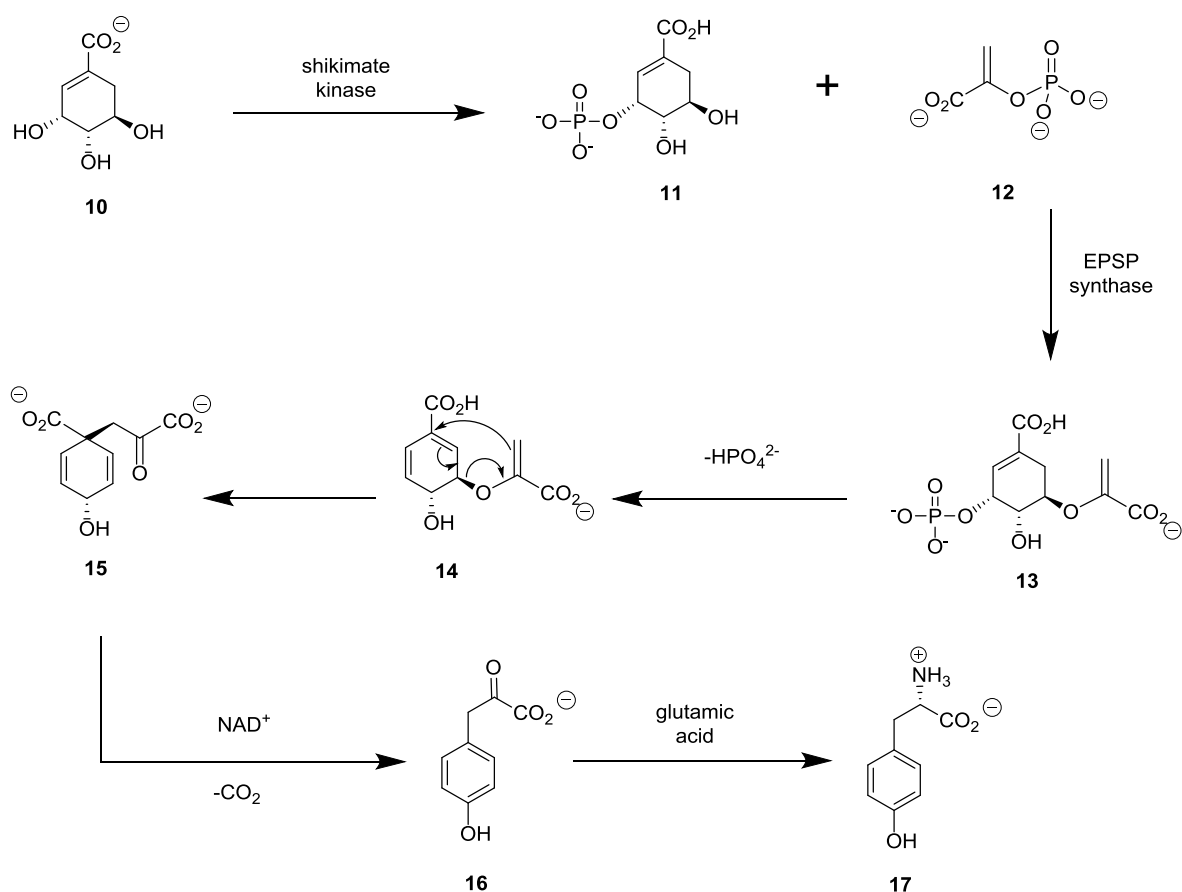
Figure 2 - neolignans

The pathway starts with the formation of 3-dehydroquinic acid (**8**) from phosphoenolpyruvic acid (**6**) and D-erythrose-4-phosphate (**7**)⁵. The enzyme DHQ synthase catalyses this reaction. The next step involves the dehydration of 3-dehydroquinic acid by the enzyme dehydroquinase to give 3-dehydroshikimic acid (**9**). A reduction then occurs of this constituent, initiated by shikimate dehydrogenase using NADP^+ as a cofactor⁶. This results in the compound shikimic acid (**10**) which is an intermediate in the synthesis of the amino acid tyrosine (Scheme 1).



Scheme 1 – biosynthesis of shikimic acid (**10**)

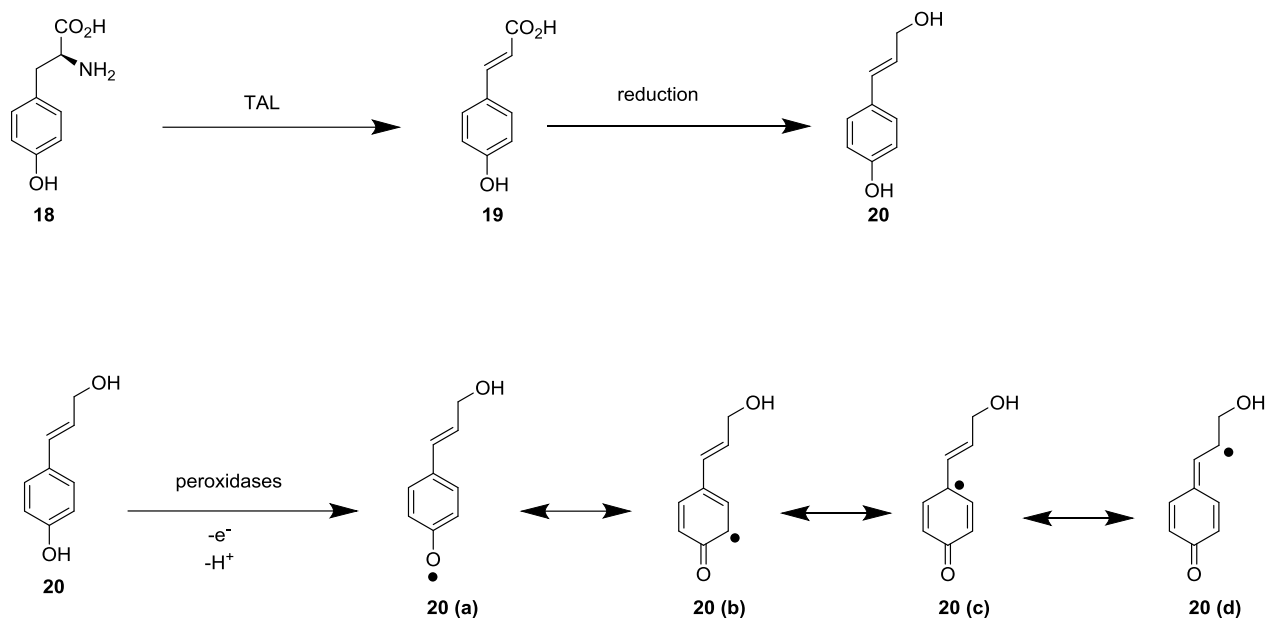
Shikimate kinase-mediated phosphorylation of shikimic acid forms product (**11**). This will then couple to phosphoenolpyruvic acid (**12**) in an EPSP synthase catalysed reaction to give compound (**13**), 5-enolpyruvylshikimate-3-phosphate. Chorismate synthase catalyzes the next reaction in which loss of the phosphate group occurs giving compound (**14**), chorismate. A rearrangement of chorismate occurs to give prephenic acid, compound (**15**). This then undergoes oxidative decarboxylation to give p-hydroxyphenylpyruvate (**16**). Tyrosine (**17**) is then obtained from the transamination of (**16**) using glutamic acid as a nitrogen source (Scheme 2).



Scheme 2 – biosynthesis of amino acid tyrosine (**17**) via shikimic acid pathway

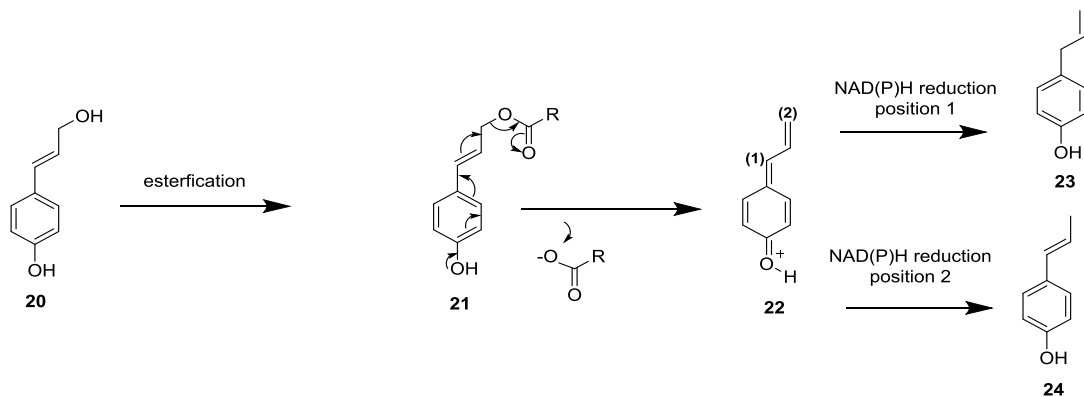
It is at this stage that *L*-tyrosine (**18**) undergoes catalytic elimination giving the 4-coumaric acid product (**19**) and subsequent reduction to 4-hydroxycinnamyl alcohol (**20**). This compound can undergo one electron oxidation to give 4 resonance hybrids. These hybrids (**20 (a)** (**b**) & (**c**)) can undergo phenolic

coupling to give dimerized products of neolignans (Scheme 3). Hybrid **(20 d)** would undergo dimerization to give a lignan rather than a neolignan.



Scheme 3 – transformation of *L*-tyrosine (**18**) to 4-hydroxycinnamyl alcohol (**20**) & one electron oxidation of (**20**) with resonance hybrids.

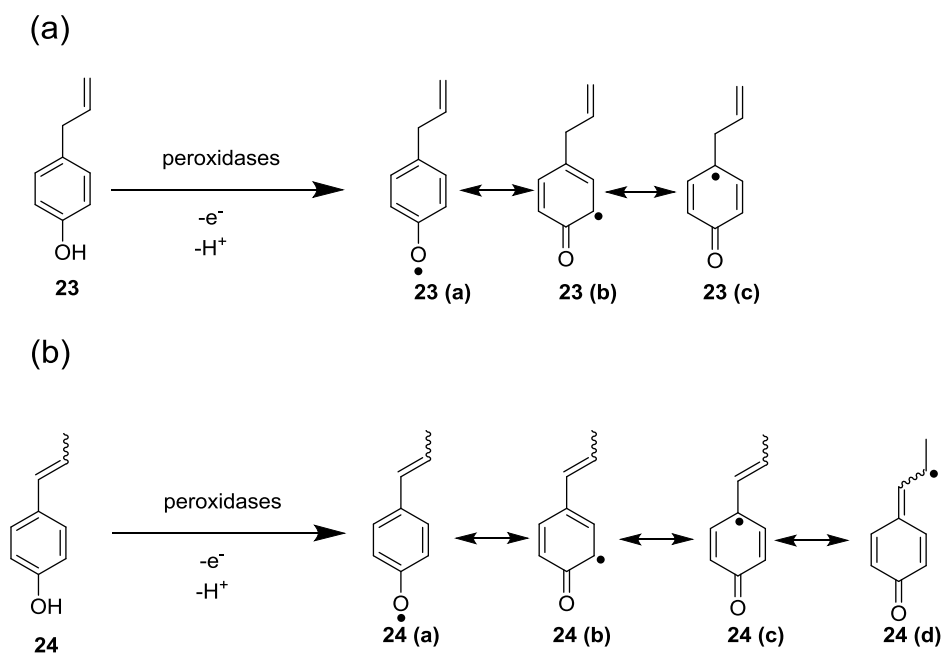
There is evidence to show that 4-hydroxycinnamyl alcohol (**20**) could be esterified from *in vitro* studies by the Lewis group ⁷ to give coumaryl ester (**21**) which subsequently decomposes to give the dienone (**22**). If reduction by NAD(P)H were to occur at position 1 indicated on dienone (**22**), the phenol would form with the alkene being placed in the terminal position giving the product chavicol (**23**) (Scheme 4).



Scheme 4 – 4-hydroxycinnamyl alcohol (**20**) esterification and pathway to chavicol (**23**) and *p*-anethole (**24**) via reduction

Chavicol can also undergo one electron oxidation and from its resonance hybrids undergo dimerization to form neolignans (Scheme 5 (a)). Examples of neolignans derived from chavicol include magnolol, honokiol and dunnianol.

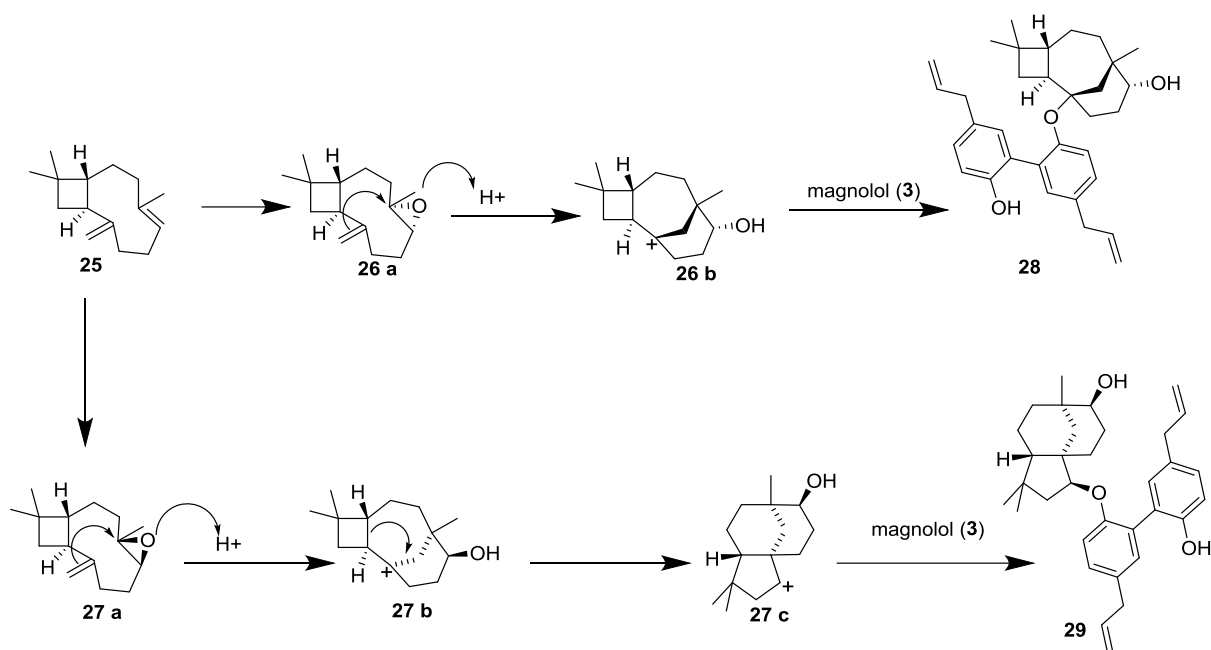
If dienone (**22**) were to be reduced by NAD(P)H at position 2, the terminal alkene, *p*-anethole (**24**) will be formed (Scheme 4). This puts the alkene in conjugation with the phenolic ring. Again, one electron oxidation of *p*-anethole will result in formation of different radical species that could then dimerize to form a variety of lignans and neolignans (Scheme 5 (b)).



Scheme 5 – oxidative coupling partners for classical lignans and neolignans

The biosynthesis of terpene containing neolignans has been investigated by the Siegel group. As mentioned, Siegel's group worked to isolate the compound clovanemagnolol³. The group also proposed the following biosynthetic pathway in which clovanemagnolol and caryolanemagnolol were derived from (-)-caryophyllene (**25**) (Scheme 6). This compound is oxidised giving diastereomeric epoxides α -caryophyllene oxide (**26 a**) and β -caryophyllene oxide (**27 a**). Upon Brønsted acid activation of each, an intramolecular attack of the external cyclic alkene occurs, resulting in the formation of the tricyclic intermediates with bridged carbocations. Tricyclic intermediate (**26 b**) couples with magnolol forming caryolanemagnolol (**28**). The intermediate (**27 b**) has the orbitals of the cation correctly aligned to allow

ring expansion of the cyclobutane portion, reducing ring strain upon formation of cationic tricyclic intermediate (**27 c**). This then couples with magnolol to form clovanemagnolol (**29**).



Scheme 6 – biosynthetic pathway to caryolanemagnolol (**28**) and clovanemagnolol (**29**)³.

1.3 Biological activity of neurite outgrowth – Neolignans and their derivatives

1.3.1 Neolignans biological activity

The thesis thus far has discussed the biological pathway in which lignans, neolignans and some of their derivatives are synthesised in nature. The following section focuses on the biological activity of neurite outgrowth, a property associated with the branching and growth of neurons within the body to facilitate the growth of an extensive and complex architecture that makes up the nervous system and brain. Many of the compounds that will be discussed have neuroprotective and neurotrophic activity. This makes these small molecules compelling as alternatives to neurotrophic factors, proteins and peptides that help promote neurite outgrowth and repairing of damaged neurons. This will possibly help in providing alternative therapies in the fight against many neurodegenerative diseases such as Alzheimer's disease and other forms of dementia.

Particular focus has been on the molecules, magnolol, honokiol and dunnianol for their neurotrophic abilities and promotion of neurite outgrowth. Magnolol has shown to have a 48% increase in growth

factor of hippocampal neurons based on *in vitro* studies of mice using DMSO as a control substance³. It also showed a 56% increase in embryonic cortical neurons within the same study carried out by the Siegel group. Other groups such as the Matsui group also provide evidence of magnolol's neuroprotective abilities. Magnolol showed significant decrease in age related neuronal loss in the hippocampus of senescence mice, evidencing its capability as a possible protective agent in early onset dementia⁸.

Honokiol has shown promotion of neurite outgrowth based on studies of rat cortical neurons at concentrations of 0.1 μM to 10 μM ⁹. Mechanistically, it is thought honokiol mobilization of Ca^{2+} within cortical neurons is the cause for the neurotrophic capabilities it presents. Ca^{2+} regulates many neuronal functions of which neurite outgrowth is one¹⁰.

Dunnianol, a sesqui-neolignan, has not been studied for its biological activity. But its isomer, isodunnianol (figure 3), has been studied for its promotion of neurite outgrowth in rat cortical neurons¹¹. The structural similarity of dunnianol and isodunnianol and the latter's ability of promoting neurite outgrowth, provided motivation to develop efficient total synthesis of the compound, which was carried out by the Denton group¹².

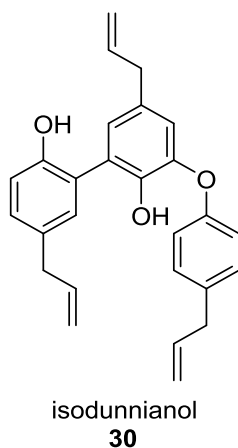


Figure 3

1.3.2 Terpene neolignans biological activity and isolation

Due to the neuronal outgrowth capabilities of the neolignans discussed, there have been further investigations into the properties of terpene containing neolignans such as caryolanemagnolol and clovanemagnolol for their own positive neuronal effects. Extensive investigations by the Fukayama

group have led to the isolation of a number of terpene-neolignans. The tables below contain summaries of these terpene containing natural products.

Table 1 - Isolation, neurotrophic activity, and total syntheses of terpene-neolignans

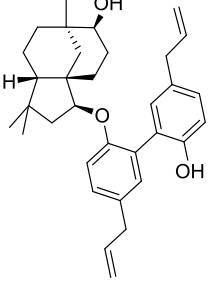
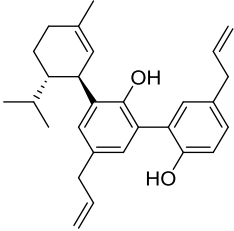
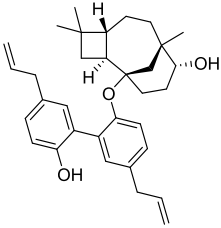
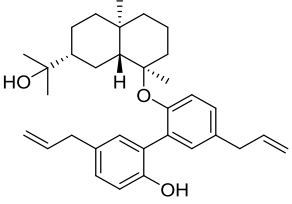
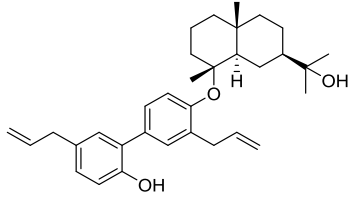
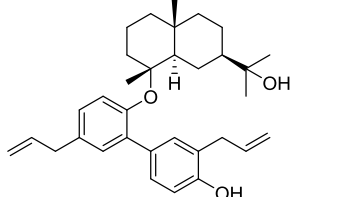
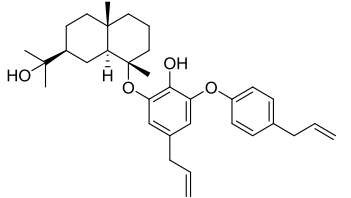
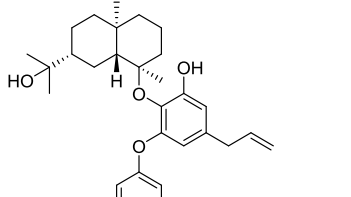
 <p>Clovanemagnolol 29</p>	<p>Isolation - <i>Magnolia Obovata</i>. 1990¹³.</p> <p>Activity - promoted neurite outgrowth of 0.1 μ M choline acetyltransferase activity (ChAT) at 1 μ M¹³. Neurite outgrowth of embryonic hippocampal neurons showed a 60% increase and a 44% growth increase of embryonic cortical neurons when subjected to clovane magnolol¹⁴.</p> <p>Synthesis: Siegel <i>et al.</i> 2010.³</p>
 <p>Monoterpenyl magnolol 30</p>	<p>Isolation - <i>Magnolia Officinalis</i> in 1991¹⁵.</p> <p>Activity - To date there have been no studies carried out on the neurotrophic capabilities of monoterpenyl magnolol.</p> <p>Synthesis: LeBel <i>et al.</i> 1995,¹⁶ Kobayashi <i>et al.</i> 2016.¹⁷</p>
 <p>Caryolanemagnolol 28</p>	<p>Isolation - <i>Magnolia Obovata</i>. 1990¹³.</p> <p>Activity - promotion of neurite outgrowth at of 0.1 μ M. At the same concentration, a 163% increase in activity of ChAT was also reported¹⁴.</p> <p>Synthesis: Siegel <i>et al.</i> 2010.³</p>
 <p>eudesmagnolol 31</p>	<p>Isolation - <i>Magnolia Obovata</i> 1990¹³.</p> <p>Activity - Less potent neurotrophic activity compared to its counterparts, even at a higher concentration of 10⁻⁵ M¹³.</p> <p>Synthesis: None reported</p>

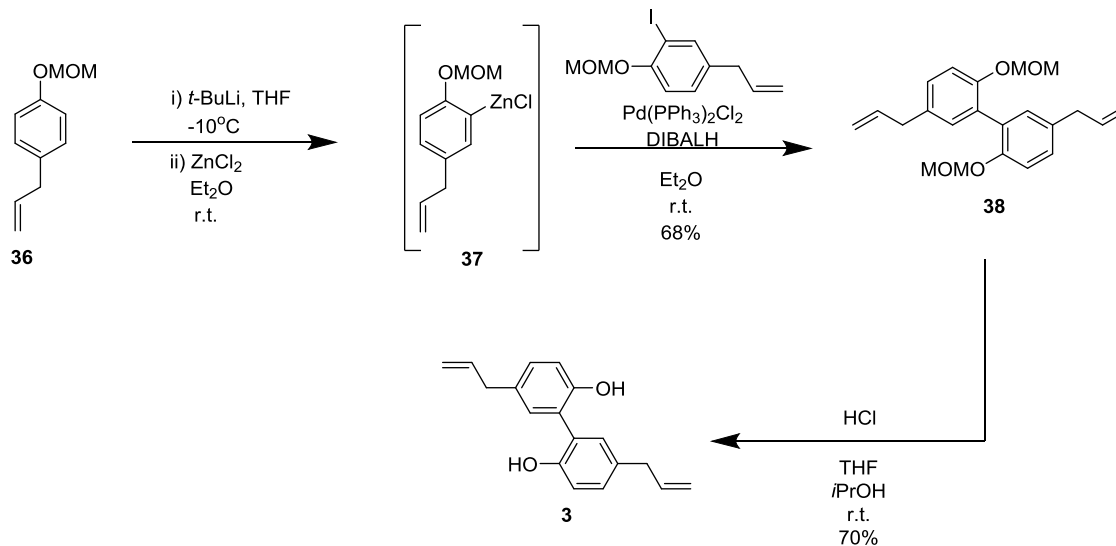
Table 2 – isolation of terpene-neolignans with no neurotrophic activity or syntheses known

 <p>eudeshonokiol A 32</p>	<p>Isolation - <i>Magnolia Obovata</i>. 1990 ¹³</p> <p>Activity – none reported</p> <p>Synthesis – none reported</p>
 <p>eudeshonokiol B 33</p>	<p>Isolation - <i>Magnolia Obovata</i>. 1990 ¹³</p> <p>Activity – none reported</p> <p>Synthesis – none reported</p>
 <p>eudesobovatol A 34</p>	<p>Isolation - <i>Magnolia Obovata</i>. 1990 ¹³</p> <p>Activity – none reported</p> <p>Synthesis – none reported</p>
 <p>eudesobovatol B 35</p>	<p>Isolation - <i>Magnolia Obovata</i>. 1990 ¹³</p> <p>Activity – none reported</p> <p>Synthesis – none reported</p>

1.4 Isolation and syntheses of neolignans

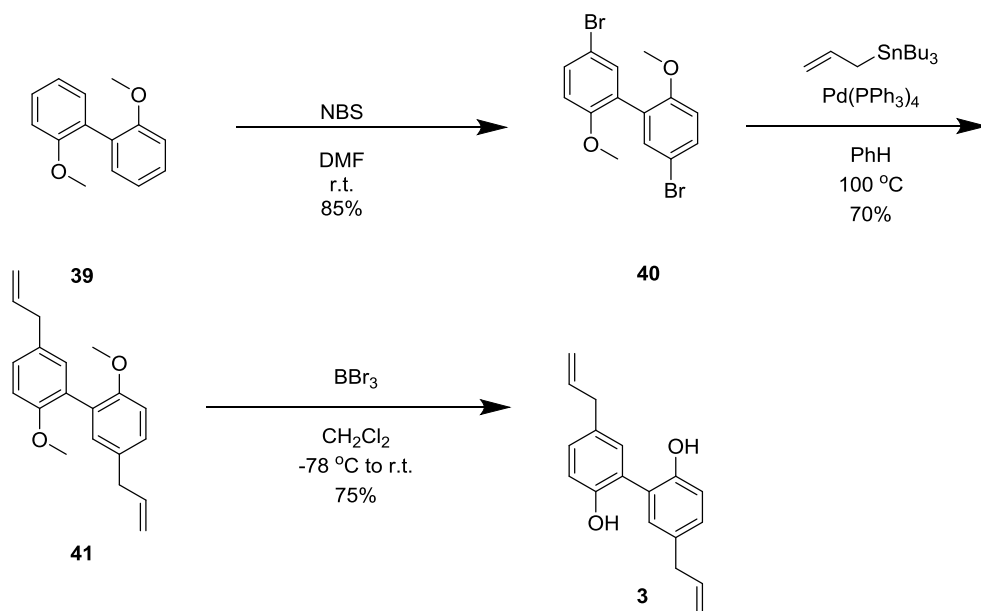
Magnolol

The neolignan magnolol (**3**) was first isolated from the bark of *Magnolia officinalis*¹⁸ and has also been isolated from the bark of *Magnolia obovata*¹⁹. The total synthesis of this compound has been carried out by a number of groups. Two strategies carried out by the Lebel group involved a Negishi cross coupling reaction and a Stille cross coupling to obtain the desired product¹⁶. The Negishi strategy involved initially the lithiation of the MOM protected substituent (**36**) and then subsequent conversion to the aryl zinc by treatment with ZnCl₂ in diethyl ether. The aryl iodide derived from the same MOM-protected intermediate undergoes reaction with the arylzinc product in the presence of palladium catalyst to afford the MOM-protected biaryl product (**38**). This was then deprotected with HCl to give magnolol (Scheme 7).



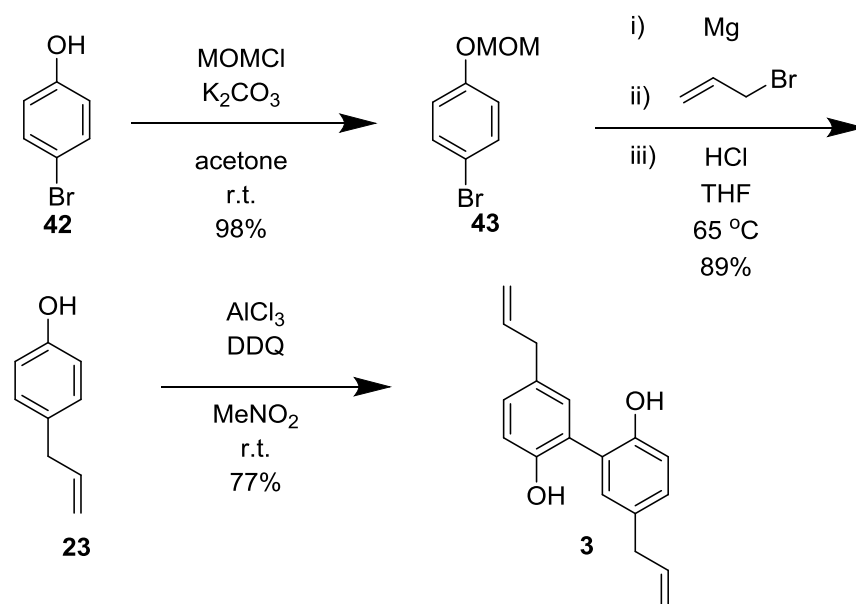
Scheme 7 Negishi strategy employed by Lebel and co-workers¹⁶

The Stille coupling was carried out on the brominated biaryl product (**40** Scheme 8) in simultaneous fashion to install the allyl groups, giving the methyl ether protected biaryl product (**41**). The ethers were then cleaved using BBr₃ to give magnolol (Scheme 8).



Scheme 8 Stille coupling strategy by LeBel and co-workers¹⁶

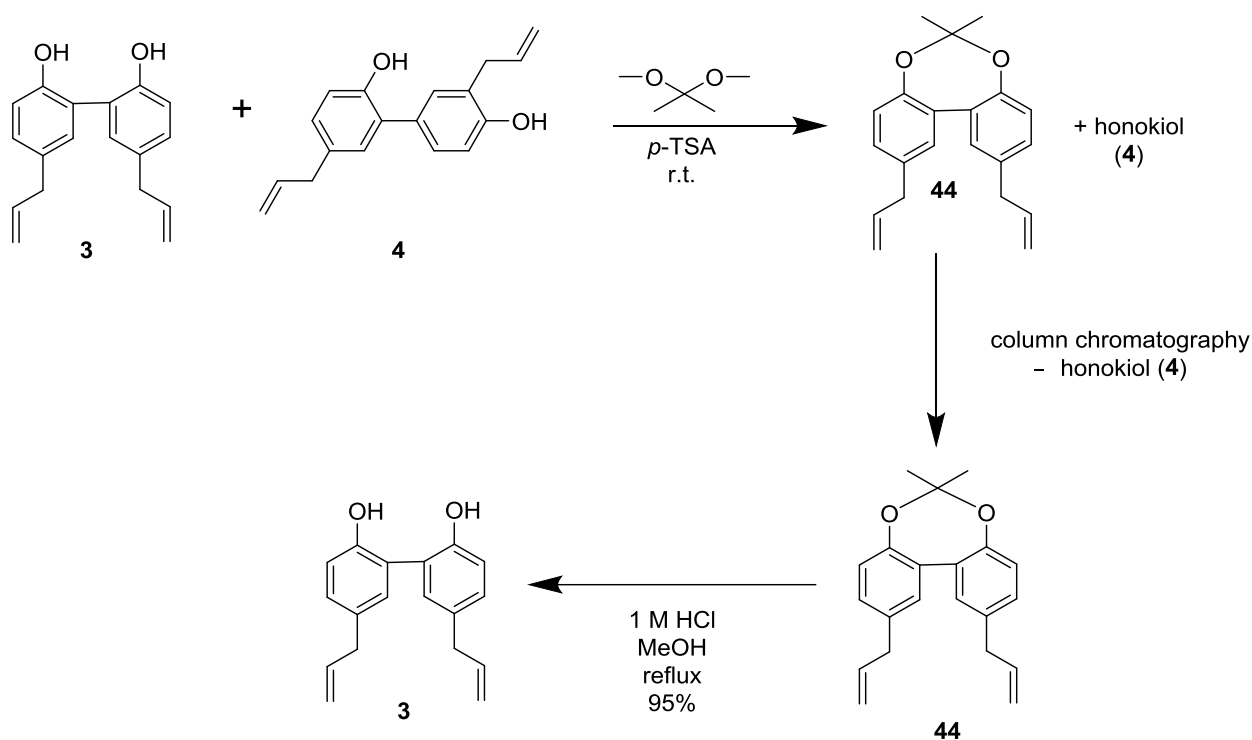
Another method carried out by the Pan group involved the protection of 4-bromophenol with MOMCl and from the product generate a Grignard reagent was generated (Scheme 9). This reagent was then reacted with allyl bromide and subsequently deprotected using HCl to give 4-allylphenol. Dimerization of this occurred through the use of oxidative coupling using DDQ as the oxidizing reagent along with AlCl_3 as a Lewis acid. This resulted in the formation of magnolol in 77% yield²⁰.



Scheme 9 – oxidative coupling strategy employed by Pan and co-workers²⁰

Another key strategy that seems to have been employed by a variety of groups in the syntheses of magnolol and other neolignans of interest is the oxidative dimerization of 4-allylphenol. The use of H₂O₂ peroxidase from horseradish resulted in dimerization of 4-allylphenol to magnolol²¹. The use of other oxidating agents in the form of FeCl₃ and K₃Fe(CN)₆ also resulted in the synthesis of magnolol²².

Each of these methods of oxidative coupling produced magnolol but also other neolignans of interest such as honokiol and dunnianol, reducing selectivity and thereby the effectiveness of this method. As magnolol and honokiol are constitutional isomers of each other, their isolation and separation has been difficult to perform. While researching the activity of honokiol's and magnolol's activity against cancer cell and HIV-1 cells, the Schinazi group developed a protection strategy in which magnolol was protected by an acetal allowing it to be separated from honokiol in high yield (Scheme 10). The protection was selective for magnolol due to the spatial arrangements in which the hydroxyl groups of both constituents are arranged. Honokiol's hydroxyl groups are too far apart to be protected in this manner²³.

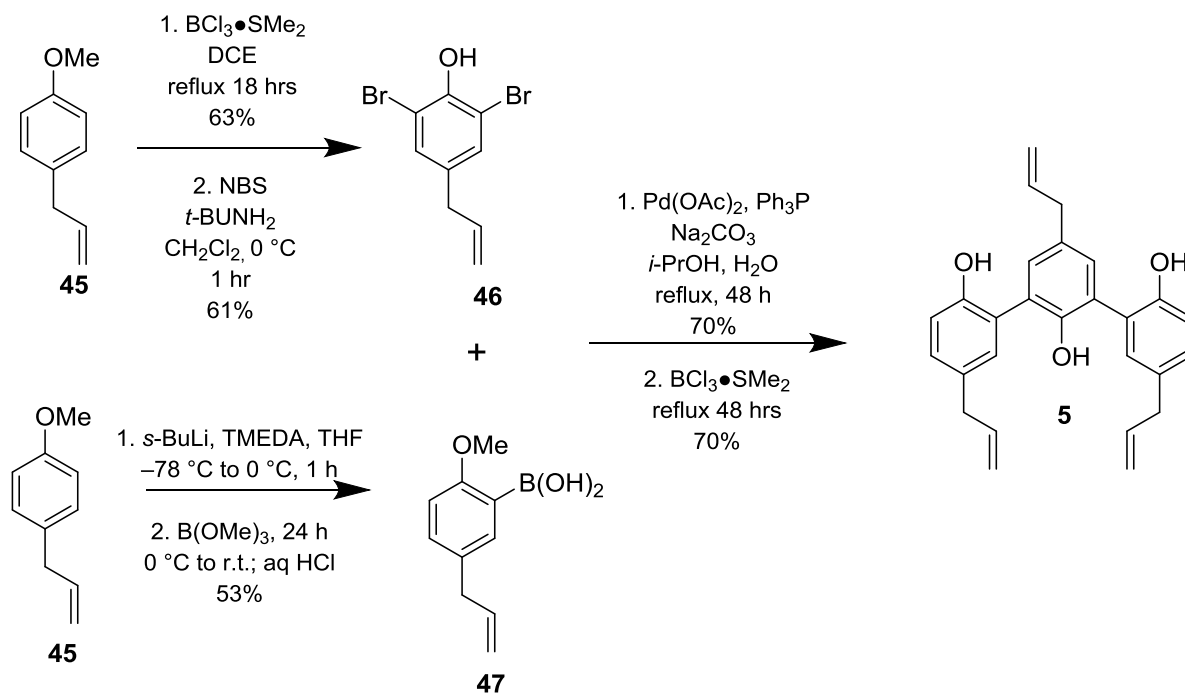


Scheme 10 – magnolol (3) protection strategy by Schinazi and co-workers²³

Dunnianol

Previous syntheses of Dunnianol have taken advantage of the oxidative dimerization methods employed by Lui and Brown resulting in yields of 1% and 11% respectively. As mentioned, the methods employed in oxidative dimerization of 4-allylphenol had little selectivity in producing the neolignans synthesised.

To date the most successful synthesis of dunnianol has been carried out by the Denton group²⁴. The strategy carried out involved a double Suzuki reaction in which initially the dibromide coupling partner (**46**) was prepared through demethylation of 4-allylanisole (**45**) using $\text{BCl}_3 \bullet \text{SMe}_2$ and subsequently brominated with NBS. The boronic acid coupling partner (**47**) was prepared via *ortho*-lithiation of 4-allylanisole and then treatment with trimethylboronate. This was then followed by hydrolysis of the boronate ester intermediate to obtain the desired boronic acid. The double Suzuki reaction was carried out using the coupling partners to obtain a methyl ether protected product. The protecting groups were then removed using $\text{BCl}_3 \bullet \text{SMe}_2$ to afford Dunnianol in 70% yield, 17% yield overall from the 4 steps carried out.



Scheme 11 – dunnianol total synthesis by Denton and co-workers²⁴

Honokiol

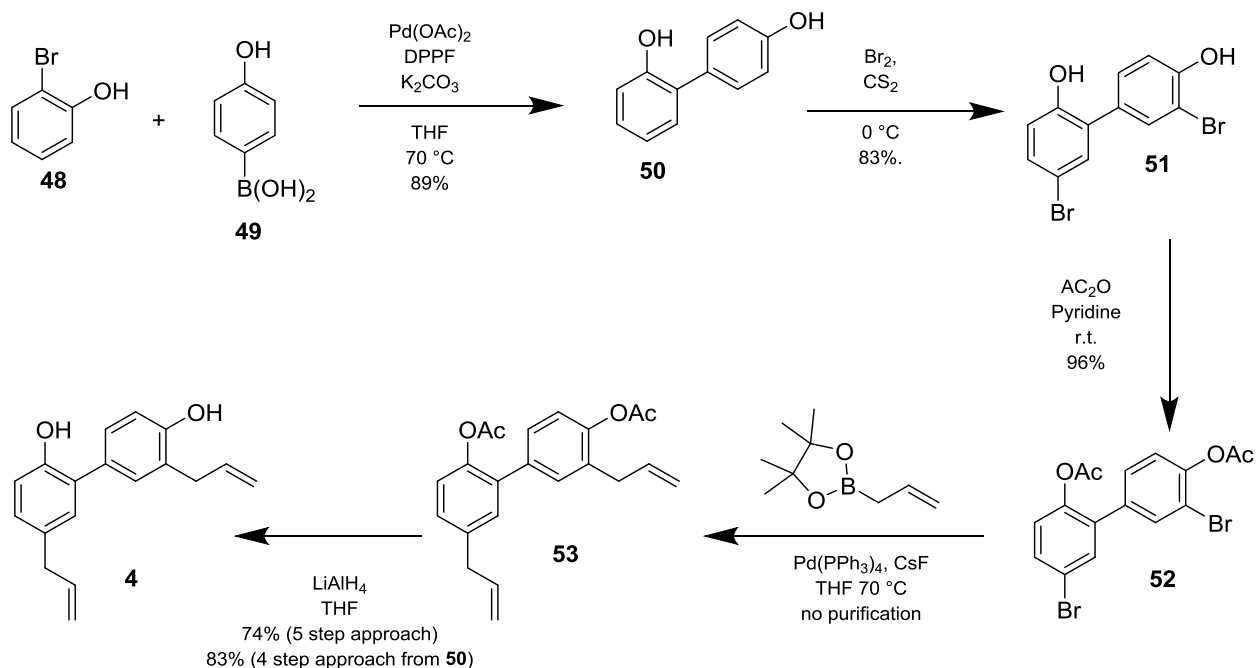
To date, Honokiol remains the most extensively synthesised of the neolignans with 9 different syntheses carried out by different research groups. These are summarised in the table below with overall yield and number of steps employed in each strategy.

Research group	key steps	Yield achieved overall
Tobinaga 1986 ²⁵	3 steps - <ul style="list-style-type: none"> Grignard addition to form biaryl bond Claisen rearrangement 	16%
Fukuyama 2004 ²⁶	14 steps – <ul style="list-style-type: none"> Suzuki cross coupling to form biaryl skeleton 	21%
Lui 2008 ²⁷	4 steps – <ul style="list-style-type: none"> Suzuki cross coupling to form biaryl skeleton 	32%
Denton 2010 ²⁸	4 steps – <ul style="list-style-type: none"> Suzuki cross coupling Allylation Claisen rearrangement. 5 steps – <ul style="list-style-type: none"> thermal Claisen rearrangement 	34% for the 4 step approach 55% for the 5 step approach
Chen 2011 ²⁹	6 steps – <ul style="list-style-type: none"> Upjohn to remove allyl group Suzuki coupling. 	45%
Fukuyama 2014 ³⁰	2 approaches employed by the group. 4 steps – <ul style="list-style-type: none"> Bromination using Br₂ 5 steps – <ul style="list-style-type: none"> Construction of biphenol 	4 step route – 83% 5 step route – 74%
Kumar 2014 ³¹	4 steps – <ul style="list-style-type: none"> Kumada cross coupling. 	68%
Reddy 2013 ³²	6 steps – <ul style="list-style-type: none"> Grignard coupling iodine mediated aromatization Claisen rearrangement. 	Conventional heating – 40% Microwave irradiation – 60%
O’Neil 2016 ³³	4 steps – <ul style="list-style-type: none"> samarium-mediated bis-benzoyl ester reduction Suzuki cross coupling 	42%

The Fukuyama group has devised the most efficient synthesis so far in preparation of honokiol. Suzuki-Miyaura reactions were employed by the group. Initially the Suzuki was carried out between 2-bromophenol (**48**) and 4-hydroxyphenyl boronic acid (**49**). This resulted in the formation of the biphenol (**50**). This biphenol is available commercially and so a synthesis was also carried out starting from this constituent. This was then brominated using Br₂ in CS₂ to yield the dibromide (**51**).

The Fukuyama group then carried out assessment of the direct coupling of this constituent using Suzuki, Kumada, and Stille reactions. It was found the dibromide constituent gave small yields of the desired product through this strategy due to low stability and reactivity to oxidative addition of Pd(0) and Ni(0) in the respective cross coupling reactions. The hydroxy groups of the dibromide were acetylated to overcome this issue, giving protected product (**52**) at 96% yield. This was then subjected to a Suzuki reaction with allylboronic acid pinacol ester to obtain the allyl product (**53**) along with monoacetylated constituents as a mixture. This mixture was subjected to LiAlH₄ without purification giving the crude honokiol product. This was then subjected to column chromatography to give the purified product in 74% overall yield.

Yield of the bromination step was increased by acetylating dibromide (**51**) without prior purification. Yield from this step improved from 63% to 83% due to this optimization. The yield obtained from the synthesis starting from the commercially available biphenol was 83% overall.



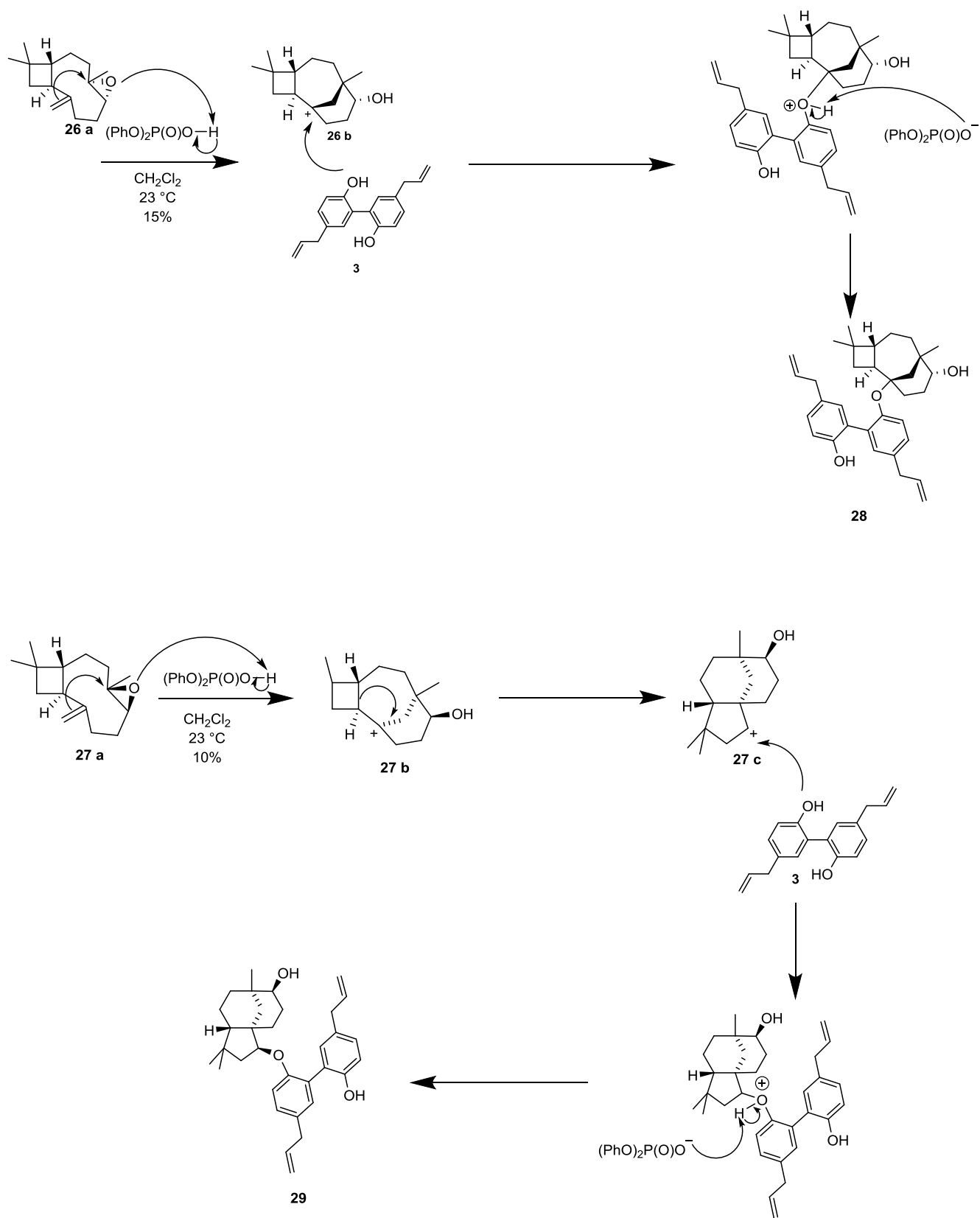
Scheme 12 – Fukuyama synthesis of honokiol (2014)³⁰.

1.5 Terpene-neolignan syntheses

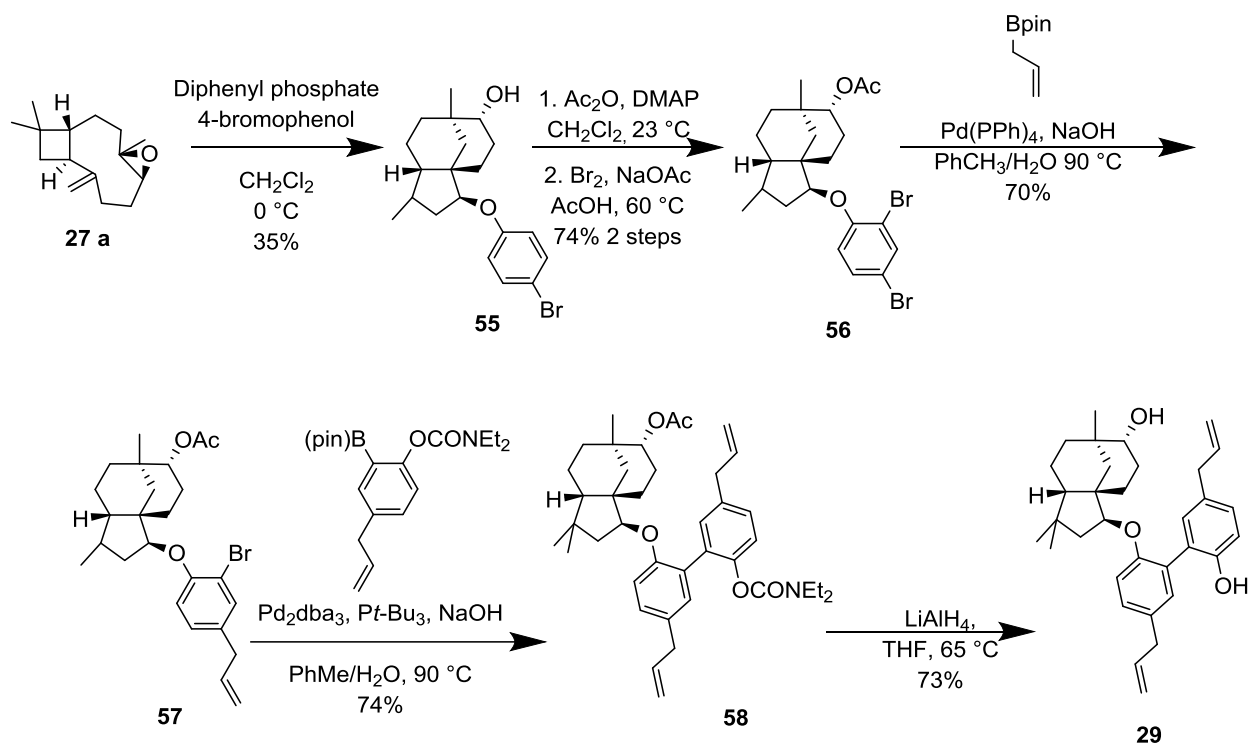
The Siegel group, upon postulating a biosynthetic pathway, developed a synthetic strategy that would lead to the synthesis of clovanemagnolol and caryolanemagnolol. Diastereoselective epoxidation of (-)-caryophyllene using *m*CPBA and Shi epoxidation was the initial step employed. This resulted in a 1:5 ratio of α -caryophyllene oxide to β -caryophyllene oxide from the *m*CPBA route. The Shi epoxidation route was more selective for α -caryophyllene oxide 2.2:1 ratio to β -caryophyllene oxide. The mixture of both epoxides was converted to clovanemagnolol and caryolanemagnolol in a single step reaction as detailed in Scheme 13³.

The group also developed multistep syntheses for clovanemagnolol and caryolanemagnolol. Scheme 14 shows the multistep synthesis for clovanemagnolol. To obtain the carbocyclic core from caryophyllene β -oxide (**27 a**), a combination of diphenyl phosphoric acid and 4-bromophenol was utilised to facilitate rearrangement. Acetylation of the secondary alcohol of (**55**) preceded treatment with Br₂ to generate dibromide (**56**). Consecutive Suzuki reactions were then utilised to bond the allyl portion of the molecule and form the biaryl bond, giving (**58**). The carbamoyl and acetate groups of (**58**) were then cleaved using LiAlH₄ to give clovanemagnolol (**29**) in 73% overall yield.

The synthesis for caryolanemagnolol followed the same procedure for clovanemagnolol with exception of the first step in which an aluminium phenoxide reagent was used to obtain the caryolanemagnolol carbocyclic core. The yield obtained for caryolanemagnolol (**28**) was 71% overall.



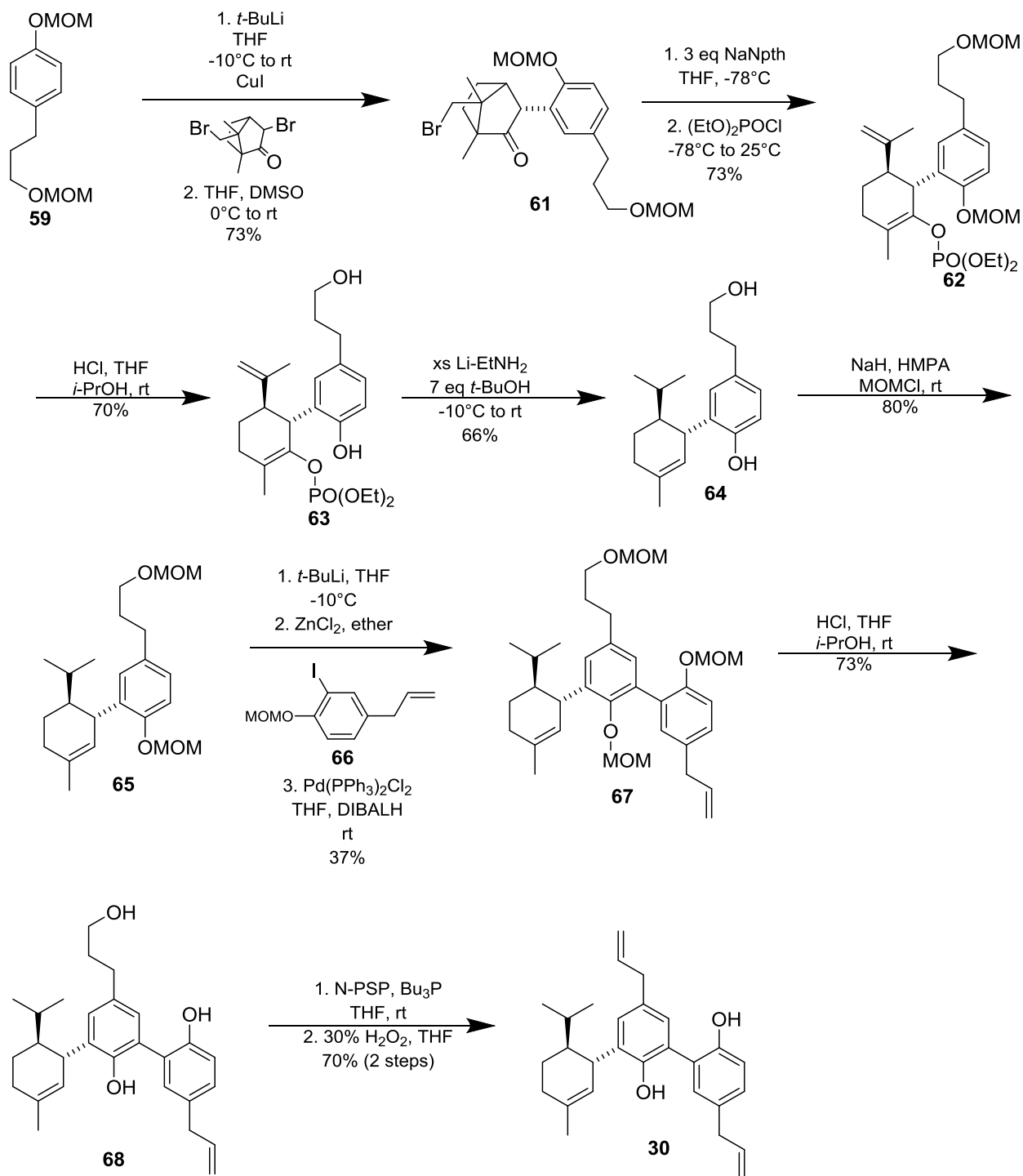
Scheme 13 – Siegel's single step reaction utilizing diphenyl phosphate³ with proposed reaction mechanisms.



Scheme 14 – Siegel's synthesis of clovanemagnolol³.

Another terpene-neolignan of interest is monoterpenylmagnolol. Two syntheses of this compound have been carried out thus far. The first started with the Lebel group¹⁶ (scheme 15). The bis(methoxymethyl) ether (**59**) was treated with *t*-BuLi and CuI to generate an organocuprate which was coupled with 3,4-dibromocamphor (**60**) to yield (**61**). This then underwent fragmentation to form (**62**) which subsequently is cleaved of its MOM groups by HCl to give (**63**). This enol phosphate was then reduced to give (**64**) in 66% yield through the utilisation of excess lithium ethylamine and *tert*-butyl alcohol.

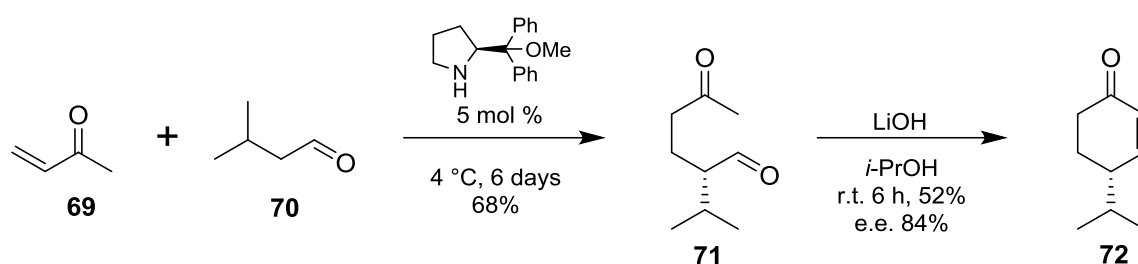
Studies carried out by the group on aryl-aryl coupling in the presence of allyl groups showed a tendency towards isomerization of the allyl constituent. To overcome this, intermediate **65** was created by MOM protection of the hydroxyl groups of (**64**). This intermediate was subjected to *tert*-butyl lithium followed by transmetalation with zinc chloride. A Negishi coupling with (**66**) provided the biaryl skeleton desired in (**67**). The cleavage of the MOM protecting groups gave (**68**) which was then treated with N-PSP. Oxidative removal of selenium derived from treatment with N-PSP using H₂O₂ gave monoterpenylmagnolol (**30**) in 70% yield.



Scheme 15 – monoterpenylmagnolol synthesis employed by LeBel and co-workers¹⁶.

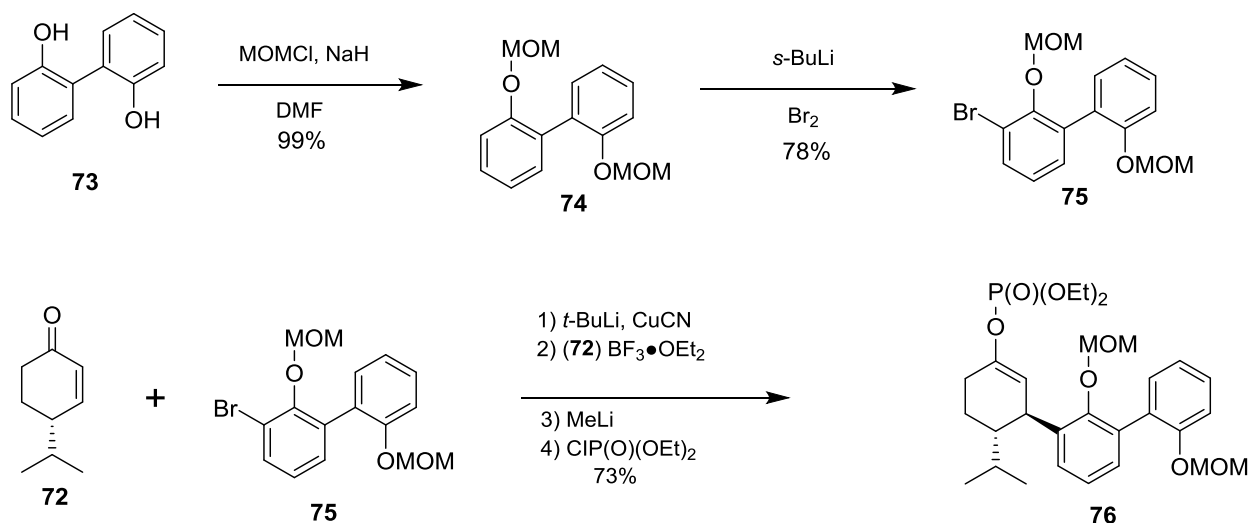
The next synthesis was carried out by the Kobayashi group using a new method of deiodination selective for the ortho position of diiodophenols¹⁷. This was started with the enantioselective synthesis of the *S* enantiomer of cryptone using the method developed by the Baran group³⁴. Methyl vinyl ketone (**69**) and

isovarelaldehyde (**70**) were combined via a Michael addition reaction and subsequently treated with base to afford cryptone (**72**) as shown in Scheme 16.



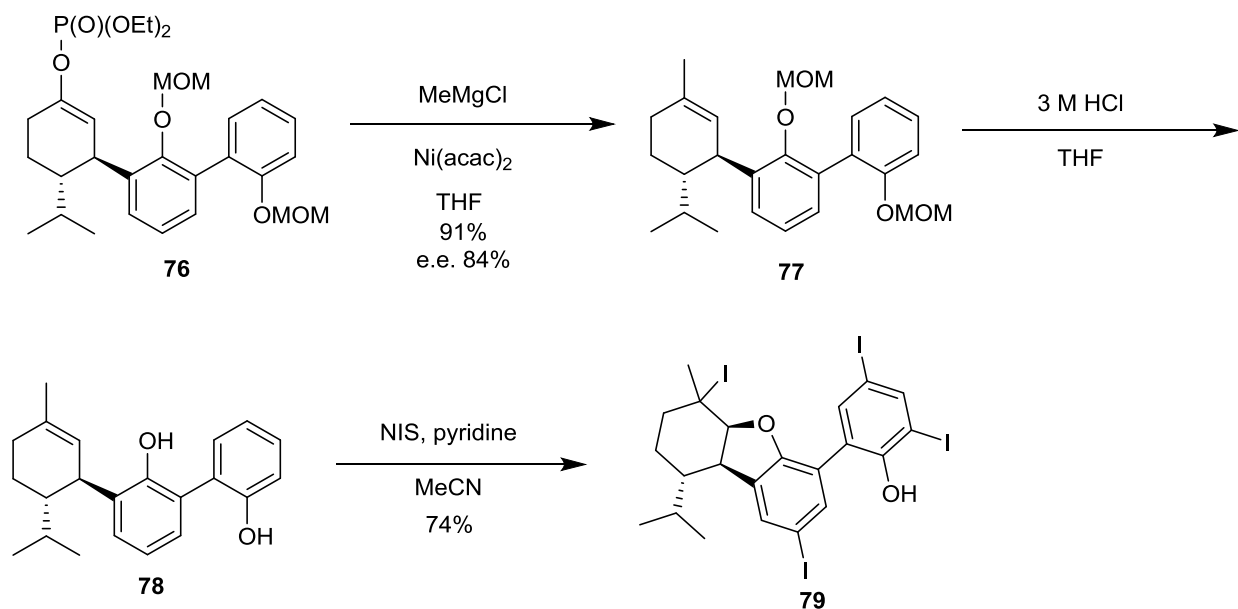
Scheme 16 – Enantioselective synthesis of cryptone employed in Kobayashi synthesis of monoterpenylmagnolol³⁴.

The group moved on to the MOM protection and bromination of 2,2-biphenol (**73**) to couple with (**72**) via an organocuprate generated by Br-Li exchange with *t*-BuLi and then treatment with CuCN (Scheme 17). A 1,4 addition to the BF₃•OEt₂ activated cryptone (**72**) to generate a boron enolate was carried out, which was subsequently treated with MeLi. This was followed by phosphorylation using ClP(O)(OEt)₂ resulting in the production of the enol phosphate (**76**).



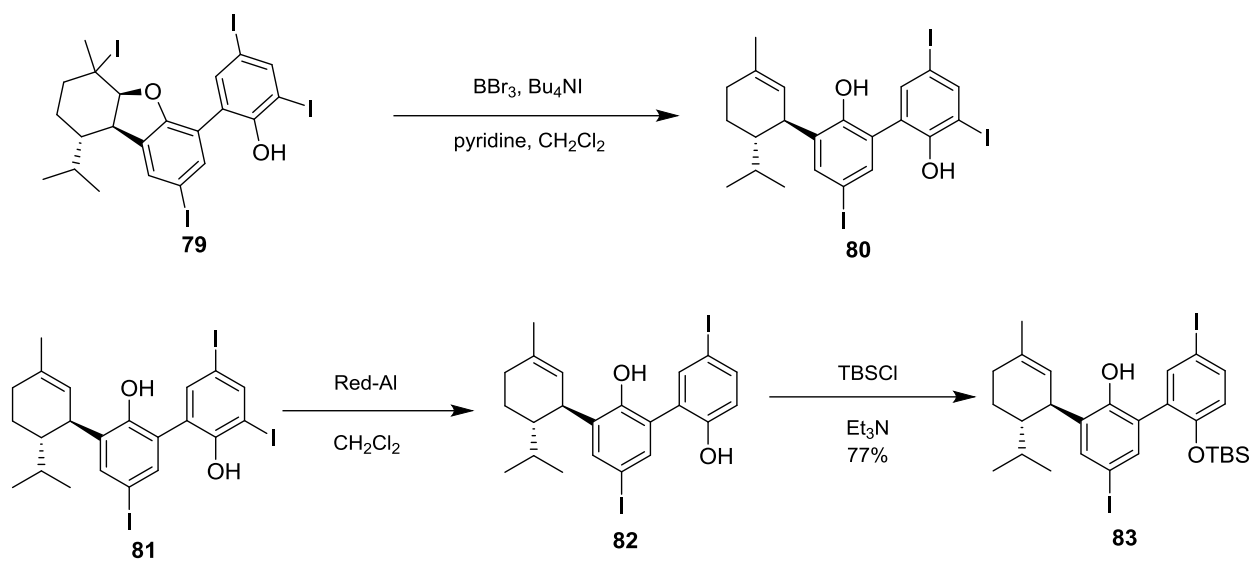
Scheme 17 – production of enol phosphate utilised in synthesis of **30**.

Continuation of the synthesis occurred with introduction of a methyl group via a Nickel-catalysed cross coupling utilising the Grignard reagent MeMgCl. Succeeding methylation was deprotection of the MOM groups using HCl to afford (**78**) (Scheme 18). The molecule was then iodinated to give constituent (**79**) using NIS. The furan resulting from this iodination was unexpected and so strategy then changed to accommodate deiodination of the ortho iodine and the terpenyl iodine of the molecule.



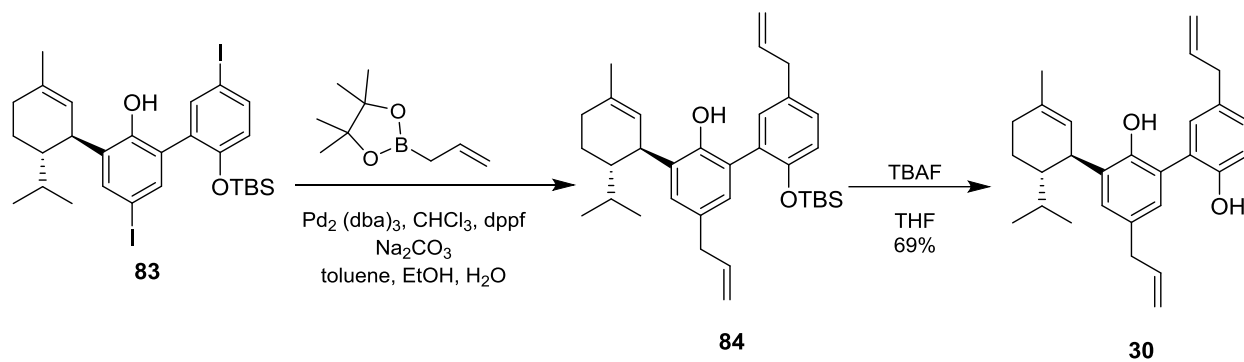
Scheme 18 – continued Kobayashi synthesis of monoterpenylmagnolol.

In removing the iodine of the terpenyl portion of the molecule, BBr_3 , Bu_4NI and pyridine were successful. The next challenge involved removal of the iodine *ortho* to the hydroxyl. The group carried out model studies using LiAlH_4 as a selective reducing agent based on previous reductions of iodobenzene to benzene. The strategy was found to have little regioselectivity and proceeded at a slow rate. They turned their attention to using Red-Al as a reducing agent which had shown excellent selectivity for *ortho* constituents in model studies. This was employed in the diiodination of (**81**) to give (**82**). An attempt at this point to install the allyl chains using allyl boronic pinacol ester resulted in an unidentifiable mixture of products. The group postulated that (**82**) chelated with Pd as bidentate ligand reducing catalytic activity. To overcome this, (**82**) was silylated to give (**83**) which would be used in the installation of the allyl groups (Scheme 19).



Scheme 19 – selective deiodination strategy using Red-Al

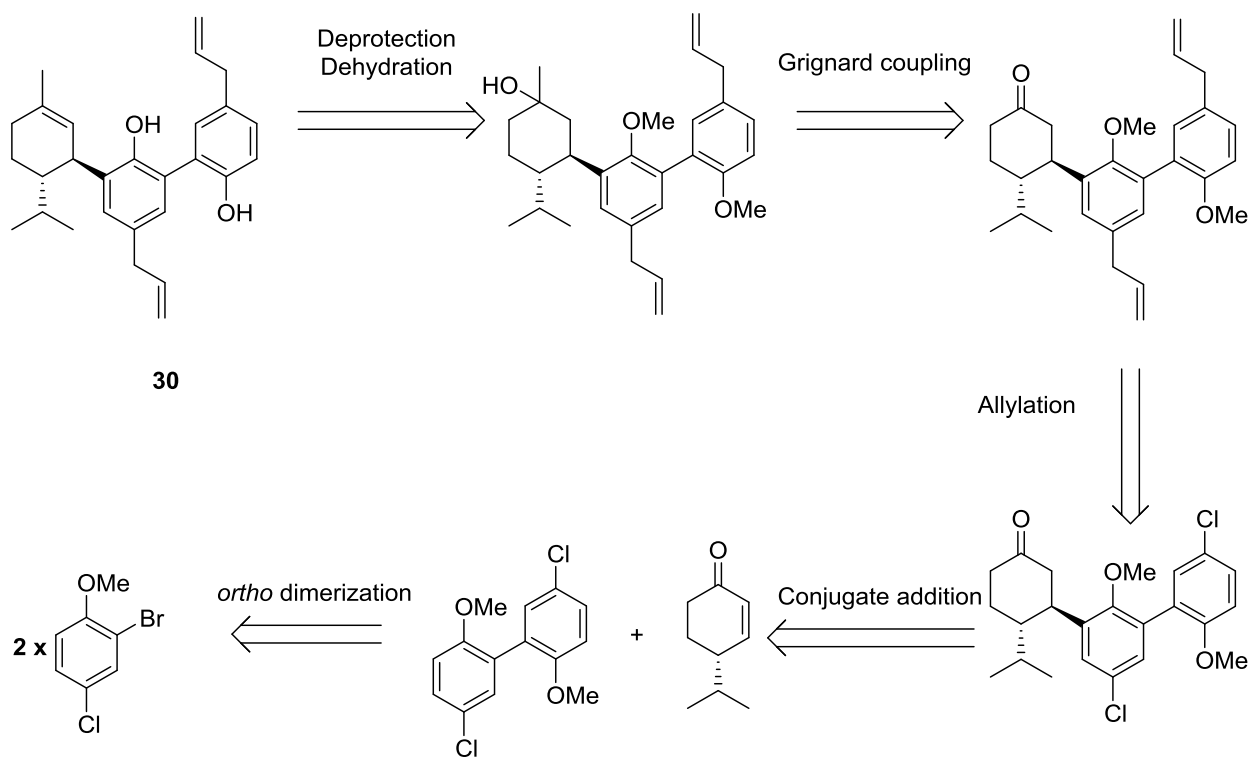
The Pd catalyzed allylation of the TBS protected product (**83**) was carried out and subsequent deprotection gave monoterpenylmagnolol (**30**) in 69% yield (Scheme 20).



Scheme 20 – allylation using pinacol boronate ester and subsequent deprotection to give monoterpenylmagnolol.

2. Project outline

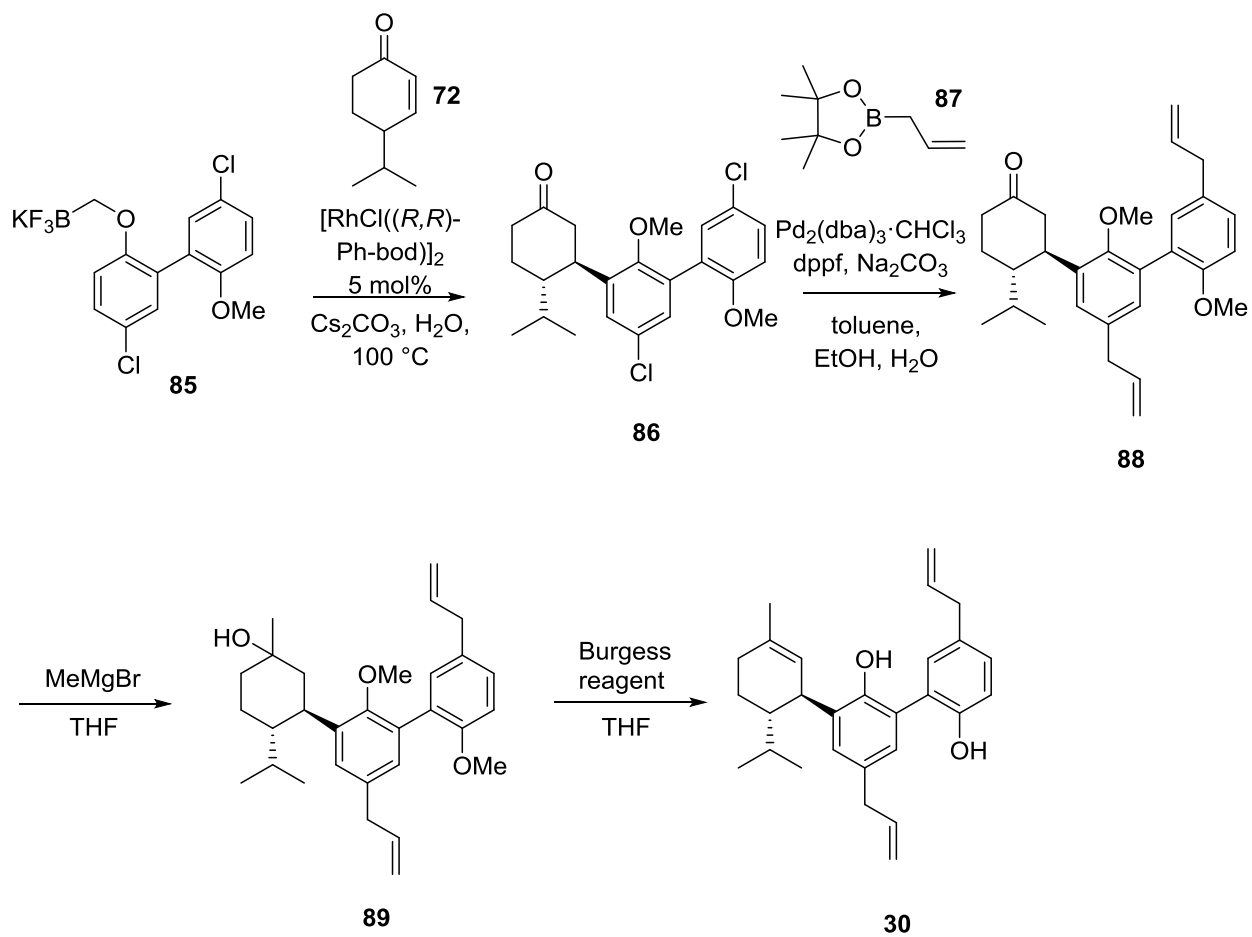
Studies into the biological effects of lignans and neolignans reveal their neuroprotective capabilities as well as other benefits such as neurite outgrowth. To study these aspects, efficient syntheses of the compounds in question must be developed. Monoterpenylmagnolol, the sesquiterpene neolignan, has been synthesised twice previously. Developing synthetic strategies into the efficient synthesis of this molecule is one aim of this project. Our retrosynthetic analysis of **(30)** (Scheme 21) took consideration of conjugate addition strategies developed by the Luo and Hayashi groups^{35,36}. Each utilised the Rh catalysed arylation of conjugated enones. These would enable addition to the cryptone constituent (**72**), which would be developed itself based on the work of the Baran group's synthesis of eudesmane terpenes³⁴. This Rh catalysed arylation of conjugated enones provides an ideal route to the arylated enone intermediate (**86**) as seen in Scheme 22.



Scheme 21 – retrosynthetic analysis of monoterpenylmagnolol

The reactivity of the allyl portion of this magnolol derivative means there is a restriction of compatible reactions that can be used in the construction of the desired molecule. Therefore, the project would start with investigations into the formation of the biaryl skeleton, with studies into the installation of the allyl group to come at a later stage. In conjunction with this work, we set out to investigate the

biosynthetic pathway hypothesised by Siegel³ for the formation of caryolanemagnolol based on computational methods utilised through Spartan 2018 suite of software.



Scheme 22 – proposed forward synthesis of monoterpenylmagnolol

3. Results and discussion

3.1.1 Construction of the biaryl skeleton

Investigation into the formation of the biaryl portion of (**85**) would begin from the constituent 2-bromo-4-chloroanisole (**90**) (figure 4). It was envisaged that coupling at the bromo constituent *ortho* to the methoxy would provide the biaryl skeleton required. The chloro constituents would provide the functionality needed to install the allyl groups via a Suzuki cross coupling with an appropriate pinacol ester such as (**87**). Appropriate methodology would be employed from the work of the Kobayashi group in this step¹⁷. Utilisation of the Ullmann reaction using methodology established by Liebeskind would provide a suitable route to the biaryl³⁷. A Turbo Grignard reagent derived from (**90**), based on Knochel's work, provides an additional method of coupling to produce the biaryl skeleton³⁸. This Grignard strategy would be used in conjunction with iron catalysed oxidative homocoupling of aryl Grignard reagents based on the work of the Hayashi group³⁹.

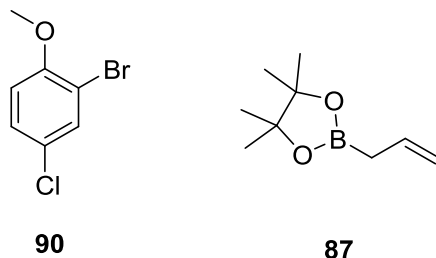
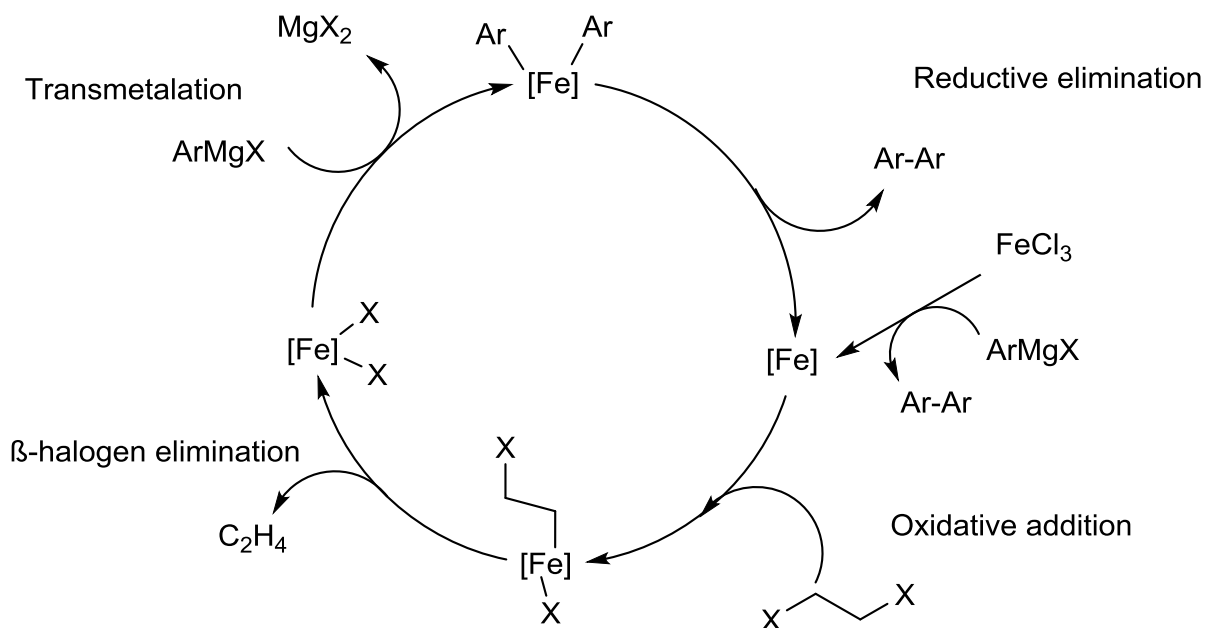


Figure 4 – 2-bromo-4-chloroanisole and allylboronic acid pinacol ester

3.1.2 Turbo Grignard route

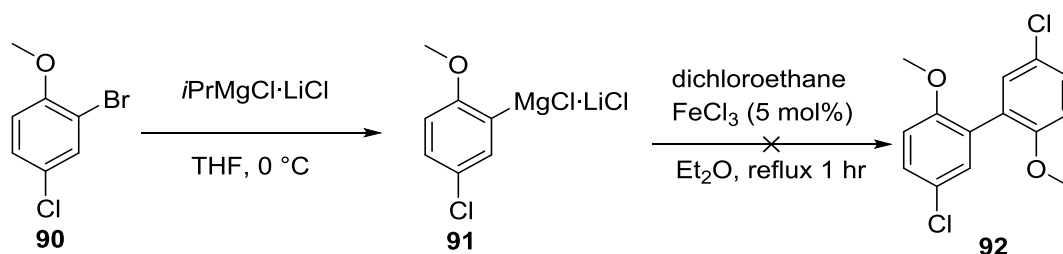
The Grignard reaction has been utilised in previous syntheses of honokiol and magnolol. The Tobinga group employed this method in formation of the biaryl backbone of honokiol²⁵. It was thought utilising the turbo Grignard reagent *i*PrMgCl·LiCl based on the work of the Knochel group³⁸ would produce the Grignard reagent required from 2-bromo-4-chloroanisole (**90**). According to studies by Knochel, this occurs through an increased rate of halogen-magnesium exchange of the bromo at the ortho position of (**90**) with the turbo Grignard³⁸. Work by the Hayashi group provided a method in which the Grignard would undergo an iron catalysed oxidative coupling to produce the symmetrical biaryl target required³⁹. This would proceed with oxidative addition of 1,2-dichloroethane to the resulting low valent iron

complex generated from the reaction of FeCl_3 with the aryl Grignard. The mechanism proposed by the Hayashi group is shown in Scheme 23.



Scheme 23 – proposed mechanism of Fe catalysed oxidative homocoupling of Grignard reagents.

The strategy began with the generation of the aryl Grignard as shown in Scheme 24. After 3 hours the reaction mixture was subjected to FeCl_3 with 1,2-dichloroethane in Et_2O and refluxed for 1 hour. Upon workup, TLC and ^1H NMR, it was found that a complex mixture of unknown species had been produced. Purification of the reaction mixture using column chromatography did not yield the desired product. Due to significant time constraints on the project, focus shifted to an alternative strategy to develop the biaryl motif.

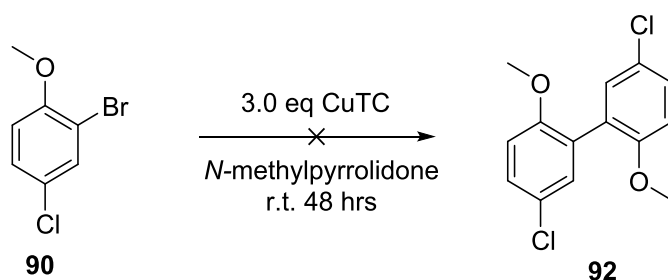


Scheme 24 – turbo Grignard and oxidative homocoupling of aryl constituents

3.1.3 Ullmann strategy

After the unsuccessful iron catalysed homocoupling of the aryl constituent, the Ullmann coupling was undertaken as an alternative. The Ullmann has been used extensively in the preparation of a variety of biaryl compounds with varying conditions and yields. Liebiskind and co-workers developed a method in which Cu(I) 2-thiophenecarboxylate (CuTC) was utilised as a highly active stoichiometric reagent for the coupling reaction³⁷. It was shown by Liebiskind's work that the mild conditions, selectivity for the *ortho* position of various aryl halides and the reactivity of CuTC resulted in moderate to excellent yields of biaryl species.

Consequently, the procedure to develop the desired biaryl was started with the addition of 2-bromo-4-chloroanisole (**90**) to a solution of CuTC in *N*-methylpyrrolidone (NMP), Scheme 25. After 48 hours of stirring, a ¹H NMR spectra of the crude product was taken to ascertain the success or failure of the procedure. Unfortunately, the ¹H NMR showed there had been no consumption of the starting material. The characteristic doublet peak expected at 6.90 ppm for the desired target was not present in the spectrum⁴⁰. It is possible the activation energy required for conversion was not attained.

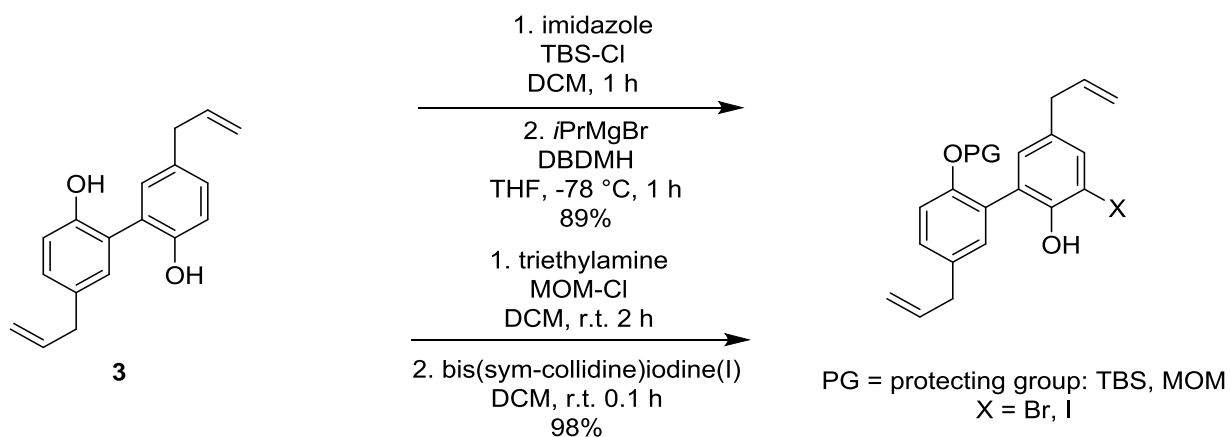


Scheme 25 – Ullmann coupling to produce biaryl motif

Ultimately, the Ullmann was carried out once more on a larger scale and temperature increased to 70 °C to see if conversion could be attained. Another ¹H NMR of the crude product was taken and illustrated the starting reactant had again not converted. The lack of success in this approach for the target molecule and significant time constraints led to adoption of alternative strategies, rather than continue with optimisation of the Ullmann approach.

3.1.4 Protection and halogenation

Due to the failures in producing the biaryl skeleton, we decided to change our strategy by starting the route to **(30)** from magnolol (**3**) itself. We postulated that mono protection of one of the hydroxyls of magnolol with subsequent halogenation of the other aryl constituent at the *ortho* position would generate a suitable coupling partner for cryptone, (**72**). The Banwell group in their synthesis of Simonsol C utilised two methods in halogenation of the *ortho* position of magnolol⁴¹. Each involved monoprotection of the hydroxyls of magnolol using either a TBS or MOM protecting group. These were then halogenated via the appropriate method as outlined in Scheme 26. These intermediates developed by Banwell and co-workers were appropriate for our needs in possibly utilising the conjugate addition chemistry we set out to apply in our synthesis of **(30)**.

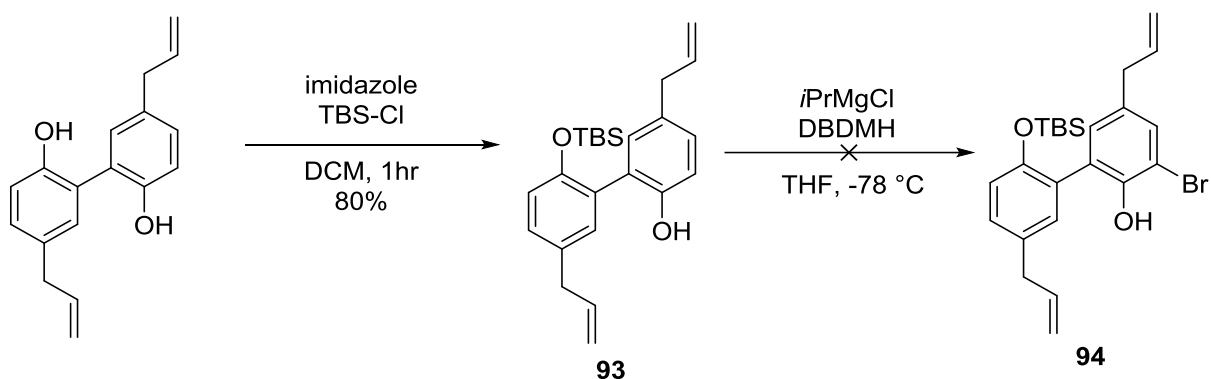


Scheme 26 – Banwell’s method to halogenated derivatives of magnolol⁴¹

3.1.5 TBS protection and bromination

In the development of Simonsol C of the *Illicium* genus a suitable method in which magnolol could be protected by *tert*-butyldimethylsilyl (TBS) and subsequently brominated using DBDMH was developed⁴¹. We employed the TBS protection successfully in our procedure (Scheme 27), but there was difficulty in the bromination step. TLC and NMR analysis showed there was a mixture of products and starting material present. It is also possible the allyl portion contributed to unwanted side reactions due to its reactivity. After a few unsuccessful attempts to overcome this through purification, it was decided the

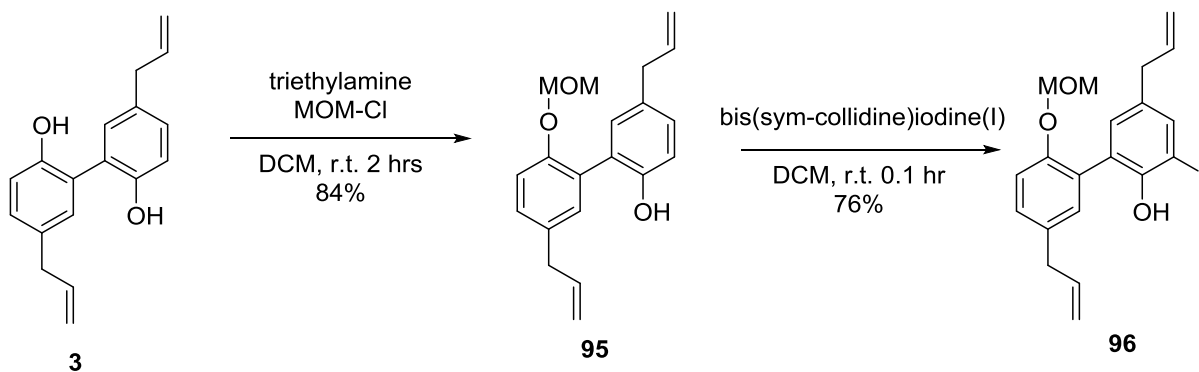
MOM protection and iodination of magnolol procedure, also developed by Banwell and co-workers, would be attempted.



Scheme 27 – TBS protection and bromination of magnolol

3.1.6 MOM protection and iodination

Magnolol was subjected to MOM-Cl to give the mono MOM protected product (**95**) (Scheme 28). This was subsequently treated with bis(sym-collidine)iodine(I) hexafluorophosphate providing the iodinated product (**96**) through donation of the iodonium ion as suggested by Rousseau's work⁴². Analysis showed that the regio- and chemoselective iodination had taken place successfully. Following this, our focus shifted to producing a suitable coupling partner.

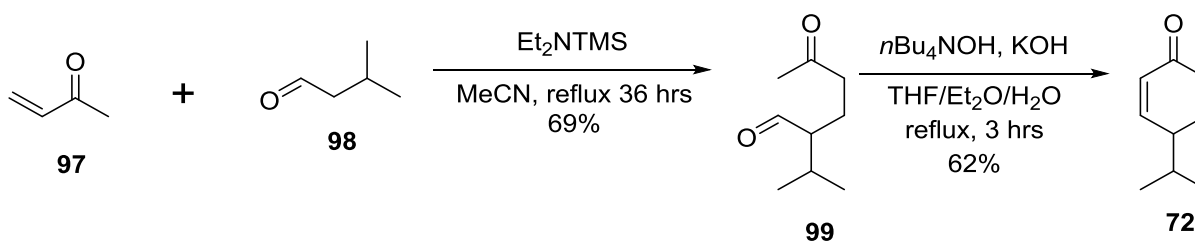


Scheme 28 – MOM protection and iodination of magnolol

3.2 Cryptone synthesis

In LeBel's initial synthesis of monoterpenylmagnolol¹⁶, the starting compound camphor, limited biological investigations due to possible analogues being produced based on its structure¹⁷. Kobayashi and co-workers sought to continue their synthesis of (**30**) using cryptone (**72**) as a coupling partner to overcome this complication. The Baran group had devised a procedure for production of the racemic version and *S*-enantiomer of cryptone³⁴. This provided the basis for which Kobayashi would continue, utilising the enantioselective synthesis.

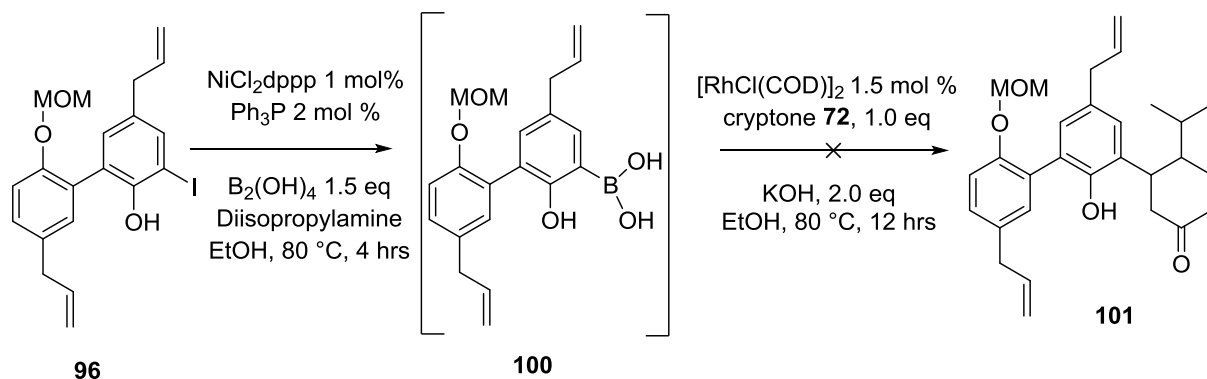
For our purposes we initially set out to produce the racemic form of cryptone using the method devised by Baran³⁴. This would proceed with the Michael addition of isovarelaldehyde (**98**) and methyl vinyl ketone (**97**) to produce racemic 2-isopropyl-5-oxohexanal (**99**) in 69% yield (Scheme 29). Upon successful synthesis of (**99**), the product was subjected to base in a phase transfer system to yield the racemic cryptone (**72**) in 62% yield.



Scheme 29 – cryptone synthesis

3.2.1 Conjugate addition strategy

Initial strategising towards coupling of the iodinated magnolol product (**96**) with the cryptone constituent (**72**) settled on a conjugate addition strategy developed by Luo and co-workers³⁵. This involved sequential borylation and Hayashi-Miyaura conjugate addition to olefins in a one pot sequence. The group reported the conversion of aryl halides to the borylated product via a nickel catalysed reaction, which according to Luo, offers a greener alternative to traditional borylations such as the Miyaura. We set out to utilise this protocol by subjecting (**96**) to the same conditions (Scheme 30).



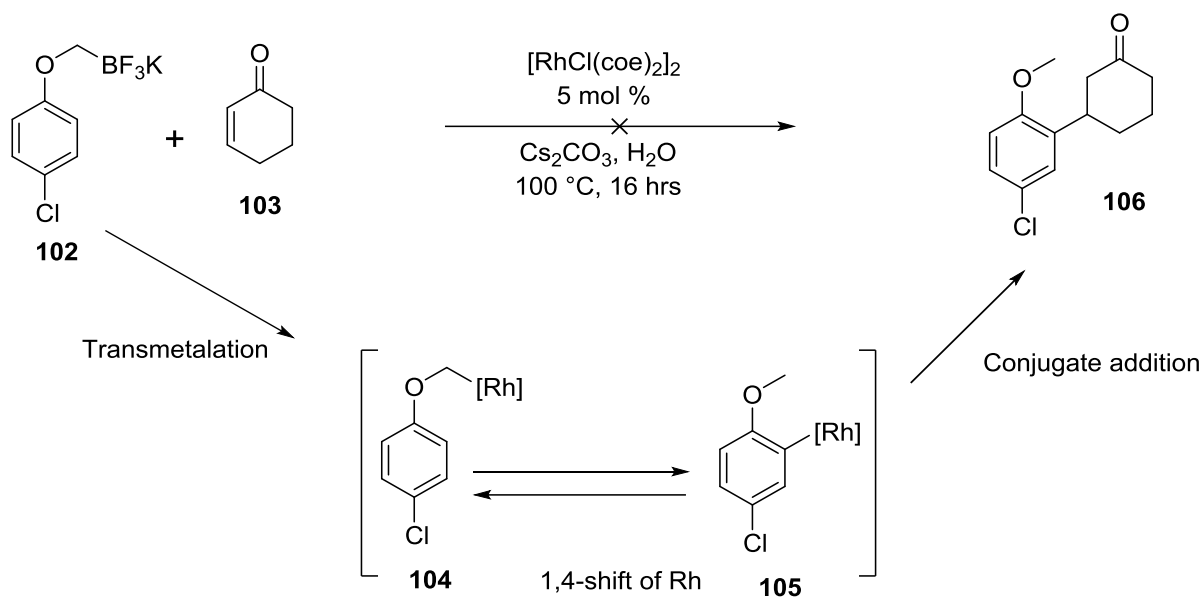
Scheme 30 – sequential borylation and conjugate addition³⁵.

Frustratingly we found that the desired product had not been produced. TLC and ¹H NMR showed there was a mixture of indiscernible products. Purification by column chromatography did not yield the desired target from this complex mixture. There are a few factors that could have contributed to the failure of this approach. It is possible the isopropyl group of the cryptone constituent provided hinderance to the reaction due to its steric interference. The complexity of the differing basic environments in the borylation step and the Rh catalysed addition step is specified within Luo's work³⁵. This may have also affected the outcome in our protocol and so further optimisation regarding the substrates in question may be needed. To ascertain if the isopropyl group was indeed the suspected hinderance to success of the addition, we decided to carry out the conjugate addition again on a more simplified substrate in cyclohexen-1-one (**103**).

3.2.2 *ortho*-Methoxyarylation through 1,4-Rhodium Shift

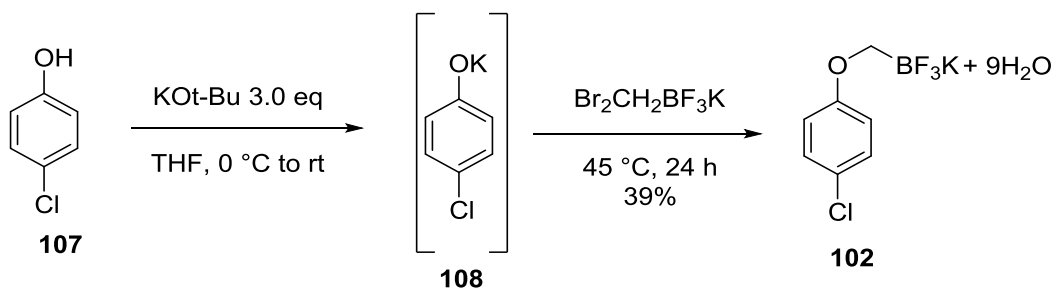
Due to the unsuccessful attempt of the sequential borylation and conjugate addition strategy, we shifted our efforts to trial studies of the arylation of conjugated enones, cyclohexen-1-one (**103**) and cryptone (**72**). The Hayashi group developed a sequence in which potassium aryloxymethyltrifluoroborates were reacted with α - β -unsaturated carbonyl compounds in the presence of a rhodium catalyst and water³⁶. The proposed mechanism of this is initially transmetalation between the boron and Rh species to create an aryloxymethyl-Rh intermediate. Subsequently, this undergoes a

1,4-shift of the Rh to the *ortho* position of the generated methoxy group to then undergo addition to an α - β -unsaturated carbonyl (Scheme 31).



Scheme 31 – proposed 1,4-shift of Rh for arylation of conjugated enones⁴³.

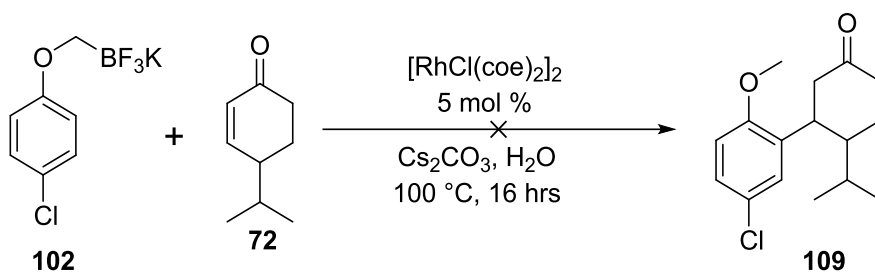
For our study we wanted to test the capability of the aryl substituents to add to cyclohexen-1-one (**103**) and cryptone (**72**). This would help establish if the isopropyl group was indeed a hindrance to the addition as speculated. It may also help distinguish if the conjugate addition is somehow hindered by the presence of another aryl species. So, we moved forward with synthesising the arylmethoxytrifluoroborate (**105**) from 4-chlorophenol (**107**). This would provide the basis with which we could perform a conjugate addition based on the protocol established by Hayashi³⁶ and provide functionality to install the allyl group at a later stage. 4-Chlorophenol was subjected to potassium *tert*-butoxide in THF to generate the intermediate (**108**). Treatment with potassium bromomethyltrifluoroborate gave the desired product (**102**).



Scheme 32 – synthesis of arylmethoxytrifluoroborate

Our first attempt at the conjugate addition proceeded with (**103**) on a small scale using the protocol established in Scheme 31. As the reaction proceeded, the mixture turned a dark brown colour. Upon analysis, we found the reaction had not produced the desired target. It is possible the Rh catalyst used under the conditions employed, did not activate as needed. Due to the small scale with which the procedure was carried out, it was difficult to assess whether catalytic activation had occurred. We decided to repeat the experiment on a larger scale along with another experiment on the same scale, but with addition of the chiral ligand (*R,R*)-Ph-Bod. It was thought that including this ligand as part of the reaction would help generate a complex *in situ* more suitable for the Rh catalysed addition. Unfortunately, the results obtained from each experiment proved to be inconsistent and did not produce the products sought. ¹H NMR in conjunction with MS analysis showed a complex mixture of inseparable compounds with no indication of starting materials present. None of the data obtained from these experiments matched the expected data for our desired targets.

Our trial studies also proceeded with the cryptone constituent in tandem with those of (**103**) (Scheme 33).



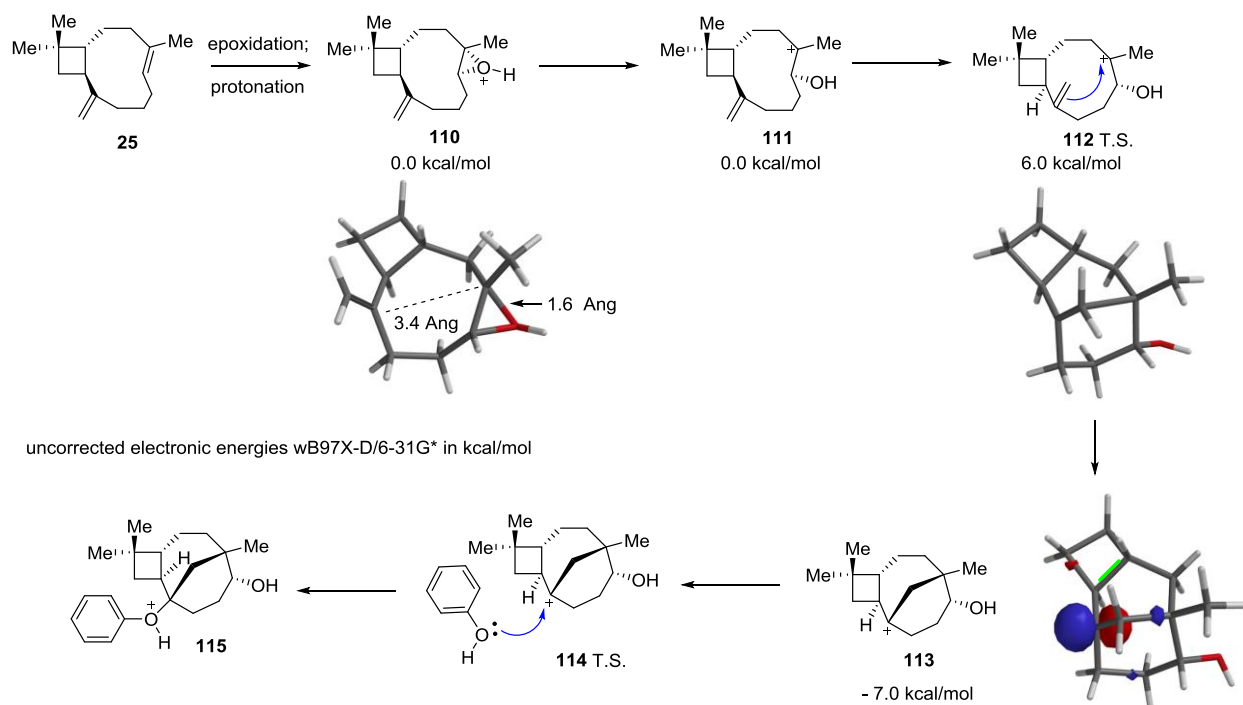
Scheme 33 – arylation of **72** through Rh catalysed conjugate addition.

Disappointingly, the desired product was again not obtained. It is probable that the isopropyl group of cryptone interfered with the reaction progress. ¹H NMR and MS experiments were also carried out for the conjugate addition of (**72**) and (**102**). Again, an unknown mixture of products was obtained based on the data presented. It is possible that the Rh complexes used in our methodology did not activate as required. Optimisation of the chiral ligands used in the conjugate additions of (**72**) and (**103**), along with the conditions used may provide a suitable avenue to reaction success in the future.

4. Computational Investigation of Biosynthetic Hypothesis For The Formation of Caryolanemagnolol

The formation of caryolanemagnolol (**28**), according to Siegel's hypothesis, most likely involves oxidation of (-)-caryophyllene (**25**) to epoxide α -caryophyllene oxide (**26 a**). This is depicted in Scheme 6 (introduction)³. To enable better understanding of this biological pathway, we carried out a computational study on the biosynthesis of (**28**). This may provide enlightenment into factors that may lead to more efficient syntheses of the compound in question. Quantum chemical calculations were employed using the Spartan 2018 suite of software. Results of this computational study are shown in Scheme 34. The ω B97X-D/6-31g* theoretical model was chosen. This was applicable as it has been used widely for the modelling of organic reactions. Calculations were carried out in the gas phase and molecular mechanics (equilibrium conformer) calculations were used on the starting materials to identify suitable conformations for the QM calculations. Transition structures were characterised by frequency calculations. These had a single imaginary frequency corresponding to the breaking/forming of bonds in the transition structure. It is thought the rearrangement reactions of this pathway are promoted by Bronsted acids. Utilising this information, we used simple protonation to generate cationic species (without a counter anion). The magnolol species was changed to a phenol species, to also aid in computational simplicity.

Caryolanemagnolol is proposed to arise from (-)-caryophyllene (Scheme 34) through epoxidation followed by Bronsted acid promoted etherification involving carbocation intermediates. The protonated epoxide (**110**) is unsymmetrical with respect to the epoxide ring with carbon oxygen bond lengths of 1.6 and 1.5 Angstroms. The longer bond length of 1.6 reflects increased carbocation character as a result of methyl substitution. In Siegel's proposed biosynthesis, the ring opening of the activated epoxide occurs through attack of the alkene portion to provide the tricyclic intermediate. In our computational investigation, we also considered epoxide opening to generate tertiary carbocation (**111**). This species was essentially isoenergetic with the protonated epoxide (energy difference of (**111**) 0.01 kcal/mol - rounded to 0.0 in Scheme 34).



Scheme 34 – computational investigation into the proposed biosynthesis of caryolanemagnolol

The transition structure of the cyclisation reaction involving the alkene (**111**) is carbocation like and indicates a very small interaction between the oxygen and the carbon atom at which the new carbon-carbon bond is forming (distance of 2.3 Angstroms). The energy barrier for the cyclisation is very low (6 kcal/mol). This means upon Bronsted acid activation, the (-)-caryophyllene epoxide will rearrange very quickly to the cation intermediate (**113**). This intermediate is found to be more stable than the (**111**) cation by 7 kcal/mol. This agrees with experimental results, as it is this species that is captured by the phenolic nucleophile (and not cation (**111**)) to give the natural product. Conformational changes of (**111**) to (**113**) results in the latter cation's increased stability over (**111**). It is believed the inability of cation (**113**) to undergo elimination, which would form an unstable bridgehead alkene in the process, results in the intermediate being long lived in the reaction medium. It is possible that 1,2-shifts of carbon-carbon bonds that make up the cyclobutene ring would occur. But the orbital overlap required for this process is unfeasible. This is illustrated by (**113**) in which the LUMO is shown. It can be seen the carbon-carbon bond highlighted in green is not positioned appropriately to overlap with the vacant orbital localised on the adjacent carbon. For these reasons the relatively stable cation (**113**) is captured by the phenol

nucleophile. In Summary, the computational analysis has established the validity of the pathway proposed by Siegel. These results provide further evidence for the inception of caryolanemagnolol.

5. Conclusions

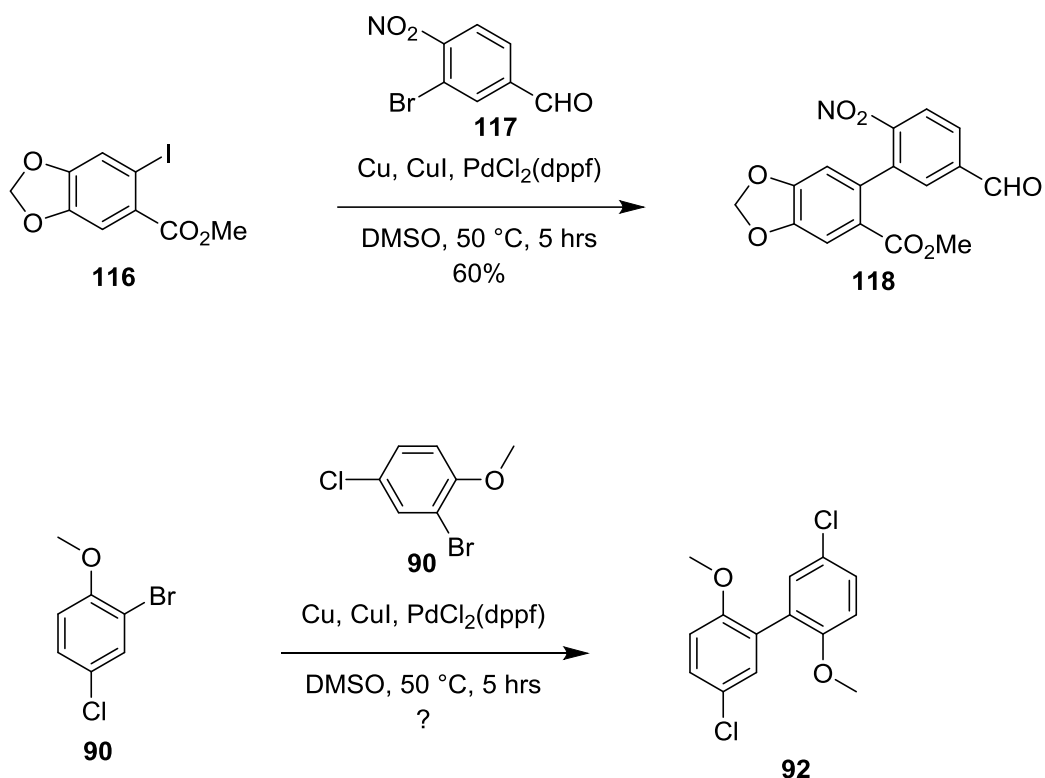
Studies towards the synthesis of the sesquiterpene neolignan monoterpenylmagnolol (**30**) have been employed using methods previously successful in syntheses of neolignans such as honokiol and caryolanemagnolol. Our aim was to try and improve upon the synthesis of (**30**), whether by increased yield, less step heavy syntheses or greener methodology. The Rh catalysed addition to *ortho*-methoxyarylated species developed by the Hayashi group still shows promise for the arylation of conjugated enones³⁶. Perhaps in alternate hands, optimisation of the reaction conditions and screening of diene ligands may lead to more appropriate Rh-complexes and yield more successful results.

In conjunction with this, a computational study on the biosynthetic pathway of caryolanemagnol has been carried out. The proposed tertiary carbocation intermediate (**111**) in our computational analysis is too unstable in respect to attack from a phenol derivative. The analysis shows the preferred cation intermediate (**113**) undergoes nucleophilic attack from the phenol derivative more readily than the tertiary intermediate. This falls in line with the studies of Siegel³.

6. Future work

The formation of the biaryl skeleton of monoterpenylmagnolol is still a factor that requires attention to enable efficient, milder and greener synthesis of the target in question. Construction of this motif has been achieved through methodologies incorporating the Suzuki, Grignard, Negishi and oxidative coupling as detailed throughout this thesis.

The Ullmann coupling, although unsuccessful in the proceeding research, could yield the desired motif if appropriate methodology is followed. The work of Banwell in constructing the unsymmetrical biaryl core of zephyrandidine III (**118**) was achieved in moderate yield using catalytic amounts of CuI and PdCl₂(dppf) in the presence of copper metal (Scheme 35)⁴⁴. These mild conditions and use of co-catalyst could possibly lead to more success in our construction studies of the biaryl motif and so should be optimised further.



Scheme 35 – Banwell’s construction of biaryl skeleton⁴⁴ and possible method for construction of neolignan biaryl core.

In adapting a greener methodology, there is potential to carry out photocatalysed coupling. Ullmann type reactions have been carried out previously with the use of photocatalysts such as Pd@TiO₂. Utilisation of this catalyst in cross coupling studies in the Scaiano group showed preferential formation of biaryls through the use of aryl iodide derivatives. The results were promising with excellent yields and mild conditions used. The reusability of the photocatalyst is also a significant advantage of this methodology⁴⁵. More recently, transition metal free photocatalysed oxidative coupling of phenol derivatives has been reported utilising MesAcr⁺BF₄⁻ as the required catalyst⁴⁶. Mechanistic studies carried out by the Kozłowski group postulate an oxidation of a phenol by the photocatalyst (**119**) followed by neutral nucleophilic addition of the corresponding phenol derivative. The benefits of this method include very mild conditions, diverse range of phenol derivatives and excellent selectivity.

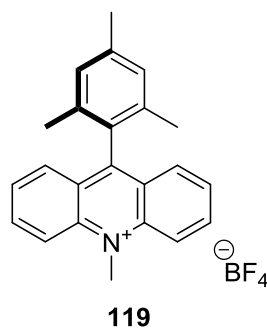


Figure 5 – photocatalyst MesAcr⁺BF₄⁻

Consideration should also be afforded to the installation of the allyl groups. Suzuki type reactions have been utilised previously in the installation of the allyl tail to the biaryl motif¹⁷. The Knochel group has developed protocols in which zinc or magnesium were inserted into aryl halides. Subsequent reaction with allyl bromide in the presence of Cu catalysts resulted in allylation of the aryl derivatives⁴⁷. Literature precedence for installation of allyl groups to aryl motifs is extensive and so full justice to the protocols that could possibly be utilised cannot be given here.

Work towards synthesis of monoterpenylmagnolol should continue through the methods discussed in this report. Significant time constraints to laboratory procedures has meant optimisation of the conditions used has not been realised. Further consideration could also be given to biosynthetic pathways of other terpene containing neolignans and the validity of their proposed mechanisms through computational analysis, as has been established within this report with caryolanemagnolol (**28**).

7. Experimental

7.1 General Details

Cooling to $-78\text{ }^{\circ}\text{C}$ was achieved using dry ice/acetone mixtures. Degassing was achieved by purging nitrogen through the solution for 5-10 min. Petrol used refers to the fraction with bp $40\text{--}60\text{ }^{\circ}\text{C}$. Commercial solvents were used as supplied. Commercial reagents were used as supplied. Analytical Thin Layer Chromatography (TLC) was carried out on Merck aluminium-backed silica gel 60 F254 plates. Developed plates were visualised using ultra-violet light (254 nm) and/or KMnO_4 solution as appropriate. Flash chromatography was performed using Fluorochem silica gel 60, $35\text{--}70$ micron. Infrared spectra were recorded neat on a Bruker ALPHAFT-IR Spectrometer. ^1H and ^{13}C NMR spectra were recorded on either Bruker AscendTM 400 or Bruker AscendTM 500 instruments as dilute solutions in the indicated deuterated solvent. All chemical shifts (δ) are reported in parts per million (ppm) relative to residual solvent peaks. All chemical shifts are reported relative to CHCl_3 ($\delta_{\text{H}}=7.27$ ppm and $\delta_{\text{C}}=77.1$ ppm). Coupling constants (J) are reported in Hertz (Hz) and are recorded after averaging. The multiplicity of a ^1H NMR signal is designated by the following abbreviations: s=singlet, d=doublet, t=triplet, m=multiplet or combinations thereof. Mass spectra were acquired on a Bruker MicroToF II instrument. All experimental procedures and spectroscopic data are given in the numerical order that the compound appears in the text of this report.

7.2 Synthesis of compounds

4-isopropylcyclohex-2-en-1-one – (72)

A solution of 2-isopropyl-5-oxohexanal (500 mg, 3.2 mmol) in diethyl ether (30 mL) and THF (10 mL) was stirred at room temperature for 15 minutes. To this solution was added 0.1 M aq solution of KOH (30 mL) and *n*Bu₄NOH (0.5 mL 40% aq) in one portion. The resulting mixture was heated at reflux for 3 hours. The mixture cooled to room temperature and was then treated with 1 M HCl solution (3 mL). The organic phase was then extracted with diethyl ether (20 mL). The combined organic layers were dried over MgSO₄ and evaporated under reduced pressure. The crude reaction mixture was subjected to column chromatography (gradient 10:1 to 5:1 petrol/diethyl ether) yielding the pure product as a light yellow oil (275 mg, 2.00 mmol, 62%). **¹H NMR** (400 MHz, CDCl₃) δ 6.90 (dt, *J* = 10.3, 2.0 Hz, 1H), 6.02 (dd, 1H, *J* = 10.3, 2.7 Hz), 2.51 (dt, *J* = 16.6, 4.3 Hz, 1H), 2.41 – 2.24 (m, 2H), 2.06 – 1.94 (m, 1H), 1.92 – 1.69 (m, 1H), 0.97 (t, *J* = 6.4 Hz, 6H). **¹³C NMR** (126 MHz, CDCl₃) δ 200.2, 154.4, 129.7, 42.5, 37.4, 31.5, 25.3, 19.7, 19.5. **IR:** ν_{\max} cm⁻¹ 3032, 2957, 2873, 1677, 1387, 1213, 831 **HRMS:** (ESI⁺)*m/z* calculated for C₉H₁₄O_na 161.0937, *m/z* found 161.0930

All data consistent with literature⁴⁸.

5,5'-diallyl-2'-((tert-butyldimethylsilyl)oxy)-[1,1'-biphenyl]-2-ol- (93)

To a solution of magnolol (**3**) (1.00 g, 3.76 mmol) and imidazole (272 mg, 4.00 mmol) in CH₂Cl₂ (40 mL) was added *tert*-Butyldimethylsilyl chloride (623 mg, 4.14 mmol) in one portion. The resulting mixture was stirred at room temperature for 1 hour and then treated with NH₄Cl (30 mL of a saturated aqueous solution). The organic phase was then extracted with CH₂Cl₂ (20 mL). The combined organic phases were dried over MgSO₄ and evaporated under reduced pressure. The crude reaction mixture was subjected to column chromatography (9:1 cyclohexane/ethyl acetate) yielding the pure product as a light yellow oil (1.15 g, 3.02 mmol, 80%). **¹H NMR:** (400 MHz, CDCl₃) δ 7.13 (d, *J* = 2.3 Hz, 1H), 7.09 – 7.06 (m, 2H), 7.05 (d, *J* = 2.2 Hz, 1H), 6.93 (d, *J* = 8.2 Hz, 1H), 6.89 (d, *J* = 8.2 Hz, 1H), 6.41 (s, 1H), 5.98 (m, 2H), 5.14 – 5.00 (m, 4H), 3.37 (t, *J* = 1.5 Hz, 4H), 0.83 (s, 9H), -0.05 (s, 6H). **¹³C NMR:** (101 MHz, CDCl₃) δ 152.1, 149.9, 138.1, 137.5, 134.6, 132.3, 132.2, 131.0, 130.1, 129.3, 129.0, 127.0, 120.6, 117.8, 115.9, 115.3, 39.5, 39.4, 25.4, 18.0, -4.74. **IR:** ν_{\max} cm⁻¹ 3394, 2954, 2928, 2857, 1638, 1492, 1256, 1229, 909, 875, 838 **HRMS:** (ESI⁺)*m/z* calculated for C₂₄H₃₂O₂SiNa 403.2064, *m/z* found 403.2060

All data consistent with literature⁴¹.

5,5'-diallyl-2'-(methoxymethoxy)-[1,1'-biphenyl]-2-ol – (95)

To a solution of magnolol (**3**) 1.00 g, 3.76 mmol) and triethylamine (530 mg, 5.25 mmol) in CH₂Cl₂ (30 mL) was added methoxymethyl-chloride (710 mg, 8.82 mmol) in one portion. The resulting mixture was stirred at room temperature for 2 hours and then treated with NH₄Cl (30 mL of a saturated aqueous solution). After 15 minutes the organic phase was extracted with Et₂O (20 mL). The combined organic phases were dried over MgSO₄ and evaporated under reduced pressure. The crude reaction mixture was subjected to column chromatography (7:3 petrol/ethyl acetate) yielding the pure product as a light orange oil (0.99 g, 3.18 mmol, 84%). ¹H NMR (400 MHz, CDCl₃) δ 7.22 – 7.04 (m, 5H), 6.96 (d, *J* = 8.2 Hz, 1H), 6.05 (s, 1H), 6.03 – 5.91 (m, 2H), 5.12 (s, 2H), 5.10 – 5.02 (m, 4H), 3.43 – 3.38 (m, 4H), 3.38 (s, 3H). ¹³C NMR (101 MHz, CDCl₃) δ 151.9, 151.8, 137.8, 137.2, 135.3, 132.4, 132.4, 131.2, 129.4, 128.4, 126.0, 117.2, 116.6, 116.0, 115.6, 96.1, 56.5, 39.4. IR: V_{max} cm⁻¹ 3416, 2976, 2901, 1638, 1493, 1227, 1153, 989, 911, 817 HRMS: (ESI⁺)*m/z* calculated for C₂₀H₂₂O₃Na 333.1461, *m/z* found 333.1458

All data consistent with the literature⁴¹.

5,5'-diallyl-3'-iodo-2'-(methoxymethoxy)-[1,1'-biphenyl]-2-ol – (96)

To a solution of **96** (250 mg, 0.803 mmol) in CH₂Cl₂ (30 mL) was added (collidene)₂IPF₆ (450 mg, 0.884 mmol). The resulting mixture was stirred for 6 minutes at room temperature and then evaporated under reduced pressure. The crude reaction mix was subjected to column chromatography (2:1 petrol/ethyl acetate) yielding the pure product as an orange oil (267 mg, 0.610 mmol, 76%). ¹H NMR (400 MHz, CDCl₃) δ 7.57 (d, *J* = 2.2 Hz, 1H), 7.18 (m, 2H), 7.09 (d, *J* = 1.8 Hz, 1H), 7.03 (d, *J* = 2.1 Hz, 1H), 6.33 (s, 1H), 6.03 – 5.87 (m, 2H), 5.11 (s, 2H), 5.10 – 5.01 (m, 4H), 3.38 (d, *J* = 6.1 Hz, 2H), 3.33 (s, 3H), 3.32 (d, *J* = 2.3 Hz, 2H). ¹³C NMR (126 MHz, CDCl₃) δ 152.5, 151.2, 138.8, 137.6, 137.5, 135.4, 134.5, 132.5, 132.3, 130.2, 128.3, 126.5, 116.8, 116.6, 116.5, 96.2, 86.4, 56.9, 39.8, 39.2. IR: V_{max} cm⁻¹ 3486, 3076, 2975, 2901, 2827, 1638, 1496, 1460, 1229, 1149, 1077, 990, 913 HRMS: (ESI⁺)*m/z* calculated for C₂₀H₂₁IO₃Na 459.0428, *m/z* found 459.0424

All data consistent with literature⁴¹.

2-isopropyl-5-oxohexanal – (99)

A solution of isovaleraldehyde (2 mL, 18.23 mmol) and (diethylamino)trimethyl silane (0.69 mL, 3.65 mmol) in MeCN (60 mL) was cooled to 0 °C and stirred for 10 minutes. Methyl vinyl ketone was added dropwise over 2 minutes. The resulting mixture was heated at reflux for 36 hours. The mixture was cooled to room temperature and then evaporated under reduced pressure. The crude reaction mixture was subjected to column chromatography (gradient 10:1 to 1:1 cyclohexane/ethyl acetate) yielding the product as a light brown oil (1.96 g, 12.55 mmol, 69%). **¹H NMR** (400 MHz, CDCl₃) δ 9.62 (d, *J* = 2.7 Hz, 1H), 2.66 – 2.29 (m, 3H), 2.14 (s, 3H), 2.12 – 1.71 (m, 3H), 1.01 (d, *J* = 6.6 Hz, 3H), 0.98 (d, *J* = 6.6 Hz, 3H). **¹³C NMR** (126 MHz, CDCl₃) δ 208.0, 205.5, 57.6, 41.3, 30.0, 28.4, 20.3, 19.5, 19.4. **IR:** ν_{\max} cm⁻¹ 2961, 2718, 1714, 1368, 1238, 1166 **HRMS:** (ESI⁺)*m/z* calculated for C₉H₁₆O₂Na 179.1043, *m/z* found 179.1055

All data consistent with literature³⁴.

Potassium (4-Chlorophenoxy)methyltrifluoroborate – (102)

To a solution of potassium tert-butoxide (670 mg, 6 mmol) in THF (15 mL) was added 4-chlorophenol (770 mg, 6 mmol) at 0 °C. The resulting solution was stirred for 15 minutes and then treated with Br₂CH₂BF₃K (0.40 g, 2 mmol). The mixture was allowed to warm to room temperature over 30 minutes and then stirred at 45 °C for 24 hours. The mixture was treated with 4.5 M KHF₂ (4.5 mL) and allowed to stir for 30 minutes. The mixture was evaporated under reduced pressure to give a crude orange solid which was suspended in Et₂O and filtered to remove organic impurities. The solution was then subjected to further reduced pressure evaporation to yield the product as a white crystalline solid (162 mg, 0.78 mmol, 39%). **¹H NMR** (400 MHz, DMSO) δ 7.22 (d, 2H), 6.86 (d, 2H), 2.96 (q, *J* = 5.1 Hz, 2H). **¹³C NMR** (101 MHz, DMSO) δ 161.4, 129.2, 122.5, 116.0. **¹⁹F NMR** (376 MHz, DMSO) δ -141.70 **¹¹B NMR** (128 MHz, DMSO) δ 1.80 (d, *J* = 284.6 Hz). **IR:** ν_{\max} cm⁻¹ 3255, 2087, 1644, 1486, 1444, 1090, 974, 828 **HRMS:** (ESI⁻)*m/z* calculated for C₇H₆BClF₃O 209.0158, *m/z* found 209.0166.

All data consistent with the literature³⁶.

7.3 Computational data

Coordinates for minima and transition structures

	2		
C	1.127760	1.038175	0.237413
C	2.595798	1.047031	0.728274
H	3.181592	1.941468	0.511713
H	2.679696	0.812520	1.793069
C	2.835798	-0.212584	-0.142898
H	3.127583	0.058195	-1.162784
C	1.319489	-0.477156	-0.035986
H	3.510114	-0.984180	0.232855
C	-0.065804	1.451631	1.056200
H	1.116112	1.560393	-0.728509
H	1.140467	-1.006271	0.908790
C	0.529347	-1.143849	-1.167116
H	0.966673	-2.112289	-1.430451
H	0.549236	-0.516202	-2.062751
C	-0.883350	-1.358081	-0.690549
C	-1.866655	-0.265726	-0.649609
H	-2.727223	-0.437426	-0.003380
C	-1.163580	-2.602980	0.098335
H	-0.849820	-3.493056	-0.453626

H	-2.213350	-2.696340	0.392460
H	-0.571248	-2.556753	1.017970
C	-1.248603	1.986457	0.272626
H	-1.025754	3.003032	-0.074122
H	-2.126015	2.067172	0.923123
C	-1.606939	1.170017	-0.988979
H	-0.815700	1.239176	-1.738599
H	-2.514681	1.581891	-1.441189
C	-0.118058	1.319948	2.381481
H	-1.005895	1.585547	2.948849
H	0.735309	0.974352	2.958080
O	-1.940755	-1.165162	-1.879004
H	-2.671544	-1.808950	-1.811685

-341023.96

No imaginary frequencies

3

C	0.163202	-1.366631	-0.712927
C	-0.234109	-2.016109	-2.060952
H	0.287540	-2.933285	-2.337885
H	-1.312483	-2.178246	-2.141927
C	0.189144	-0.696636	-2.756549

H	1.253046	-0.706068	-3.014555
C	-0.063269	0.002615	-1.404980
H	-0.388208	-0.353884	-3.616996
H	1.245144	-1.516259	-0.599288
H	-1.135599	0.227871	-1.343411
C	0.752913	1.217370	-0.949312
H	0.705060	2.020891	-1.691380
H	1.803883	0.940836	-0.825754
C	0.446203	1.051173	1.631325
H	-0.258595	1.274255	2.432020
C	0.345729	-1.447427	1.837343
H	1.016268	-2.311592	1.920094
H	-0.274225	-1.448489	2.740271
C	1.252637	-0.196145	1.826361
H	2.016838	-0.272842	1.049715
H	1.775419	-0.117178	2.784718
O	1.304361	2.275821	1.325175
H	0.996232	3.063009	1.813333
C	0.169344	1.712814	0.347448
C	-0.524880	-1.599794	0.605501
C	-1.825511	-1.872801	0.707460
H	-2.452215	-2.016709	-0.168153
H	-2.311358	-1.993525	1.671808

C	-1.000466	2.648870	0.262910
H	-1.350762	2.984656	1.243754
H	-1.827650	2.110726	-0.211117
H	-0.763628	3.512716	-0.364051

-341023.95

No imaginary frequencies

4

C	-1.364999	-0.202966	-0.817536
C	-2.129050	0.076407	-2.147443
H	-3.053564	-0.481002	-2.299315
H	-2.304945	1.142721	-2.311535
C	-0.846733	-0.417794	-2.888538
H	-0.852584	-1.504402	-3.009772
C	-0.095368	0.040870	-1.622660
H	-0.580784	0.059191	-3.832117
H	-1.463992	-1.281373	-0.647360
H	0.055078	1.120387	-1.730591
C	1.148494	-0.534560	-0.908772
H	2.044582	-0.346016	-1.511064
H	1.036131	-1.610546	-0.755657
C	1.064203	-0.551470	1.706268

H	1.139500	0.165840	2.532986
C	-1.460362	-0.394630	1.728129
H	-2.373410	-0.994553	1.657394
H	-1.536046	0.216902	2.632768
C	-0.240062	-1.330440	1.825803
H	-0.269546	-2.105663	1.053391
H	-0.232620	-1.854054	2.785417
O	2.162787	-1.450555	1.687947
H	2.878450	-1.108214	2.239638
C	1.289360	0.185261	0.393244
C	-1.305614	0.479688	0.510173
C	-0.823394	1.738963	0.640203
H	-0.665896	2.394597	-0.211091
H	-0.699637	2.189464	1.621515
C	2.168447	1.382537	0.418645
H	3.195974	0.991236	0.495160
H	1.992661	2.032003	1.277455
H	2.122938	1.952170	-0.512686

-3410117.96

One imaginary frequency i131 which when animated corresponds to the correct forming/breaking carbon-carbon bonds.

5

C	-1.443862	-0.234038	-0.831261
C	-2.217124	-0.022438	-2.189051
H	-3.127370	-0.614719	-2.277608
H	-2.421746	1.032062	-2.382227
C	-0.922256	-0.511700	-2.900508
H	-0.884288	-1.603223	-2.950903
C	-0.178965	0.067429	-1.681792
H	-0.690547	-0.087022	-3.876951
H	-1.545622	-1.312793	-0.652140
H	-0.161284	1.146174	-1.869363
C	1.081779	-0.288271	-0.906481
H	1.977097	-0.018481	-1.472990
H	1.140103	-1.362609	-0.711424
C	1.069196	-0.408964	1.683803
H	1.168140	0.242532	2.566534
C	-1.528757	-0.404189	1.689101
H	-2.383313	-1.077918	1.591260
H	-1.648680	0.234835	2.568013
C	-0.210476	-1.250232	1.828624
H	-0.201260	-2.039419	1.070750
H	-0.236932	-1.742714	2.804891
O	2.191650	-1.244751	1.547984

H	2.413538	-1.633124	2.402747
C	1.060516	0.515390	0.439680
C	-1.283419	0.389245	0.471353
C	-0.294912	1.437899	0.597169
H	-0.291342	2.191102	-0.189400
H	-0.262265	1.905576	1.581765
C	2.232221	1.498059	0.501834
H	3.162610	0.923616	0.520809
H	2.192946	2.120595	1.401120
H	2.244623	2.152090	-0.375336

-341030.94

No imaginary frequencies

8. References

- 1 R. B. Teponno, S. Kusari and M. Spiteller, *Nat. Prod. Rep.*, 2016, **33**, 1044–1092.
- 2 J. Y. Pan, S. L. Chen, M. H. Yang, J. Wu, J. Sinkkonen and K. Zou, *Nat. Prod. Rep.*, 2009, **26**, 1251–1292.
- 3 X. Cheng, N. L. Harzendorf, T. Shaw and D. Siegel, *Org. Lett.*, 2010, **12**, 1304–1307.
- 4 K. M. Herrmann and L. M. Weaver, *Annu. Rev. Plant Physiol. Plant Mol. Biol.*, 1999, **50**, 473–503.
- 5 B. A. Bohm, *Chem. Rev.*, 1965, 435–466.
- 6 K. Huang, M. Li, Y. Liu, M. Zhu, G. Zhao, Y. Zhou, L. Zhang, Y. Wu, X. Dai, T. Xia and L. Gao, *Front. Plant Sci.*, 2019, **10**, 1–12.
- 7 D. G. Vassão, D. R. Gang, T. Koeduka, B. Jackson, E. Pichersky, L. B. Davin and N. G. Lewis, *Org. Biomol. Chem.*, 2006, **4**, 2733–2744.
- 8 N. Matsui, H. Nakashima, Y. Ushio, T. Tada, A. Shirono, Y. Fukuyama, K. Nakade, H. Zhai, Y. Yasui, N. Fukuishi, R. Akagi and M. Akagi, *Biol. Pharm. Bull.*, 2005, **28**, 1762–1765.
- 9 Y. Fukuyama, K. Nakade, Y. Minoshima, R. Yokoyama, H. Zhai and Y. Mitsumoto, *Bioorganic Med. Chem. Lett.*, 2002, **12**, 1163–1166.
- 10 H. Zhai, K. Nakade, Y. Mitsumoto and Y. Fukuyama, *Eur. J. Pharmacol.*, 2003, **474**, 199–204.
- 11 M. Moriyama, J. M. Huang, C. S. Yang, H. Hioki, M. Kubo, K. Harada and Y. Fukuyama, *Tetrahedron*, 2007, **63**, 4243–4249.
- 12 R. M. Denton and J. T. Scragg, *Synlett*, 2010, **4**, 633–635.
- 13 Y. Fukuyama, Y. Otoshi, K. Miyoshi, K. Nakamura, M. Kodama, M. Nagasawa, T. Hasegawa, H. Okazaki and M. Sugawara, *Tetrahedron*, 1992, **48**, 377–392.
- 14 X. Cheng, N. Harzendorf, Z. Khaing, D. Kang, A. M. Camelio, T. Shaw, C. E. Schmidt and D. Siegel, *Org. Biomol. Chem.*, 2012, **10**, 383–393.
- 15 T. Konoshima, M. Kozuka, H. Tokuda, H. Nishino, A. Iwashima, M. Haruna, K. Ito and M. Tanabe, *J. Nat. Prod.*, 1991, **54**, 816–822.
- 16 M. R. Agharahimi and N. A. Lebel, *J. Org. Chem.*, 1995, **60**, 1856–1863.
- 17 A. Ikoma, N. Ogawa, D. Kondo, H. Kawada and Y. Kobayashi, *Org. Lett.*, 2016, **18**, 2074–2077.
- 18 Y. H. Chen, P. H. Huang, F. Y. Lin, W. C. Chen, Y. L. Chen, W. H. Yin, K. M. Man and P. L. Liu, *Eur. J. Integr. Med.*, 2011, **3**, e317–e324.
- 19 K. Ito, T. Iida, K. Ichino, M. Tsunozuka, M. Hattori and T. Namba, *Chem. Pharm. Bull. (Tokyo)*, 1982, **30**, 3347–3353.
- 20 W. Gu, X. She, X. Pan and T. K. Yang, *Tetrahedron Asymmetry*, 1998, **9**, 1377–1380.

- 21 S. C. Tzeng and Y. C. Liu, *J. Mol. Catal. B Enzym.*, 2004, **32**, 7–13.
- 22 L. K. Sy and G. D. Brown, *J. Chem. Res. - Part S*, 1998, 476–477.
- 23 F. Amblard, D. Delinsky, J. L. Arbiser and R. F. Schinazi, *J. Med. Chem.*, 2006, **49**, 3426–3427.
- 24 R. M. Denton and J. T. Scragg, *Synlett*, 2010, **4**, 633–635.
- 25 T. Takeya, T. Okubo and S. Tobinaga, *Chem. Pharm. Bull.*, 1986, **34**, 2066–2070.
- 26 T. Esumi, G. Makado, H. Zhai, Y. Shimizu, Y. Mitsumoto and Y. Fukuyama, *Bioorganic Med. Chem. Lett.*, 2004, **14**, 2621–2625.
- 27 C. M. Chen and Y. C. Liu, *Tetrahedron Lett.*, 2009, **50**, 1151–1152.
- 28 R. M. Denton, J. T. Scragg, A. M. Galofré, X. Gui and W. Lewis, *Tetrahedron*, 2010, **66**, 8029–8035.
- 29 S. Tripathi, M. H. Chan and C. Chen, *Bioorganic Med. Chem. Lett.*, 2012, **22**, 216–221.
- 30 K. Harada, C. Arioka, A. Miyakita, M. Kubo and Y. Fukuyama, *Tetrahedron Lett.*, 2014, **55**, 6001–6003.
- 31 J. Srinivas, P. P. Singh, Y. K. Varma, I. Hyder and H. M. S. Kumar, *Tetrahedron Lett.*, 2014, **55**, 4295–4297.
- 32 B. V. Subba Reddy, R. Nageshwar Rao, N. Siva Senkar Reddy, R. Somaiah, J. S. Yadav and R. Subramanyam, *Tetrahedron Lett.*, 2014, **55**, 1049–1051.
- 33 A. M. Wright and G. W. O’Neil, *Tetrahedron Lett.*, 2016, **57**, 3441–3443.
- 34 K. Chen, Y. Ishihara, M. M. Galán and P. S. Baran, *Tetrahedron*, 2010, **66**, 4738–4744.
- 35 C. Fan, Q. Wu, C. Zhu, X. Wu, Y. Li, Y. Luo and J. B. He, *Org. Lett.*, 2019, **21**, 8888–8892.
- 36 J. Ming and T. Hayashi, *Org. Lett.*, 2016, **18**, 6452–6455.
- 37 S. Zhang, D. Zhang and L. S. Liebeskind, *J. Org. Chem.*, 1997, **62**, 2312–2313.
- 38 A. Krasovskiy and P. Knochel, *Angew. Chemie - Int. Ed.*, 2004, **43**, 3333–3336.
- 39 T. Nagano and T. Hayashi, *Org. Lett.*, 2005, **7**, 491–493.
- 40 A. Kar, N. Mangu, H. M. Kaiser and M. K. Tse, *J. Organomet. Chem.*, 2009, **694**, 524–537.
- 41 J. Nugent, M. G. Banwell and B. D. Schwartz, *Org. Lett.*, 2016, **18**, 3798–3801.
- 42 Y. Brunei and G. Rousseau, *Tetrahedron Lett.*, 1995, **36**, 8217–8220.
- 43 J. Ming and T. Hayashi, 1–103.
- 44 X. Xu, H. S. Kim, W. M. Chen, X. Ma, G. J. Correy, M. G. Banwell, C. J. Jackson, A. C. Willis and P. D. Carr, *European J. Org. Chem.*, 2017, **2017**, 4044–4053.
- 45 N. Marina, A. E. Lanterna and J. C. Scaiano, *ACS Catal.*, 2018, **8**, 7593–7597.

- 46 K. A. Niederer, P. H. Gilmartin and M. C. Kozlowski, *ACS Catal.*, 2020, 14615–14623.
- 47 D. S. Ziegler, K. Karaghiosoff and P. Knochel, *Angew. Chemie - Int. Ed.*, 2018, **57**, 6701–6704.
- 48 M. E. Daub, J. Prudhomme, C. Ben Mamoun, K. G. Le Roch and C. D. Vanderwal, *ACS Med. Chem. Lett.*, 2017, **8**, 355–360.